

FINAL REPORT

Enhancement of Magnetic Data by Stable Downward Continuation for UXO Application

SERDP Project MM-1642

JUNE 2010

Yaoguo Li,
Richard Krahnenbuhl,
Sarah Devries
**Center for Gravity, Electrical, & Magnetic
Studies**
Department of Geophysics
Colorado School of Mines

This document has been approved for public release.



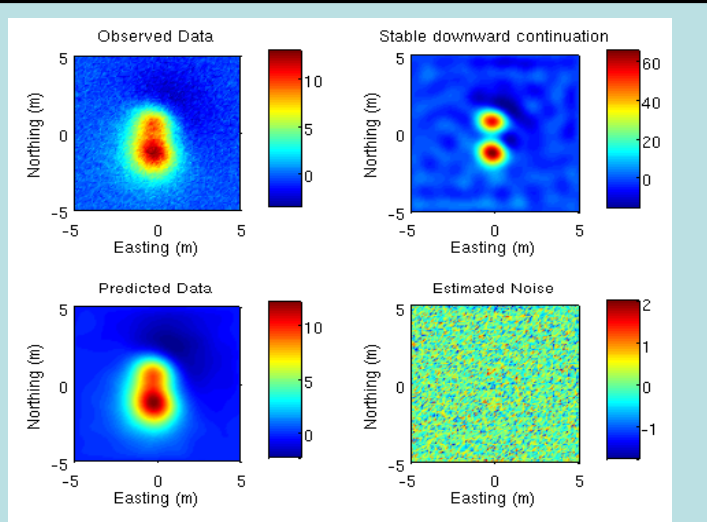
SERDP

Strategic Environmental Research and
Development Program

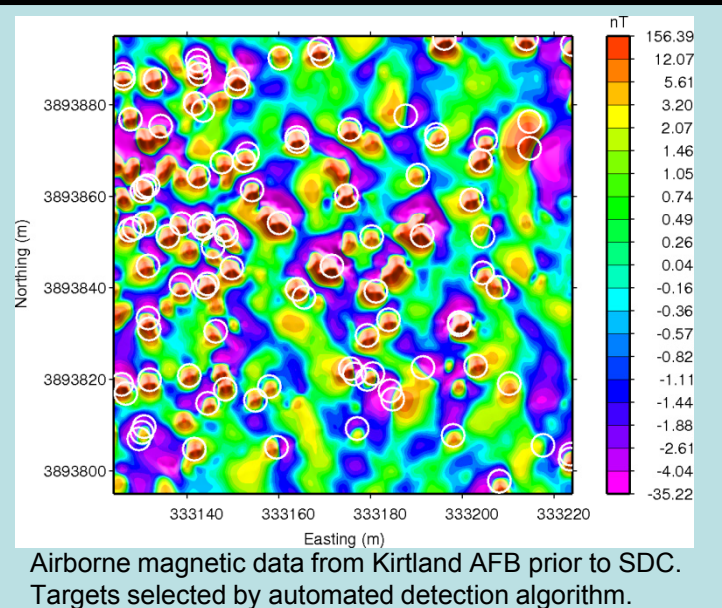
Report Documentation Page			<i>Form Approved OMB No. 0704-0188</i>	
<p>Public reporting burden for the collection of information is estimated to average 1 hour per response, including the time for reviewing instructions, searching existing data sources, gathering and maintaining the data needed, and completing and reviewing the collection of information. Send comments regarding this burden estimate or any other aspect of this collection of information, including suggestions for reducing this burden, to Washington Headquarters Services, Directorate for Information Operations and Reports, 1215 Jefferson Davis Highway, Suite 1204, Arlington VA 22202-4302. Respondents should be aware that notwithstanding any other provision of law, no person shall be subject to a penalty for failing to comply with a collection of information if it does not display a currently valid OMB control number.</p>				
1. REPORT DATE JUN 2010	2. REPORT TYPE	3. DATES COVERED 00-00-2010 to 00-00-2010		
4. TITLE AND SUBTITLE Enhancement of Magnetic Data by Stable Downward Continuation for UXO Application			5a. CONTRACT NUMBER	
			5b. GRANT NUMBER	
			5c. PROGRAM ELEMENT NUMBER	
6. AUTHOR(S)			5d. PROJECT NUMBER	
			5e. TASK NUMBER	
			5f. WORK UNIT NUMBER	
7. PERFORMING ORGANIZATION NAME(S) AND ADDRESS(ES) Colorado School of Mines, Department of Geophysics, Center for Gravity, Electrical, & Magnetic Studies, Golden, CO, 80401			8. PERFORMING ORGANIZATION REPORT NUMBER	
9. SPONSORING/MONITORING AGENCY NAME(S) AND ADDRESS(ES)			10. SPONSOR/MONITOR'S ACRONYM(S)	
			11. SPONSOR/MONITOR'S REPORT NUMBER(S)	
12. DISTRIBUTION/AVAILABILITY STATEMENT Approved for public release; distribution unlimited				
13. SUPPLEMENTARY NOTES				
14. ABSTRACT				
15. SUBJECT TERMS				
16. SECURITY CLASSIFICATION OF:			17. LIMITATION OF ABSTRACT Same as Report (SAR)	18. NUMBER OF PAGES 65
a. REPORT unclassified	b. ABSTRACT unclassified	c. THIS PAGE unclassified	19a. NAME OF RESPONSIBLE PERSON	

This report was prepared under contract to the Department of Defense Strategic Environmental Research and Development Program (SERDP). The publication of this report does not indicate endorsement by the Department of Defense, nor should the contents be construed as reflecting the official policy or position of the Department of Defense. Reference herein to any specific commercial product, process, or service by trade name, trademark, manufacturer, or otherwise, does not necessarily constitute or imply its endorsement, recommendation, or favoring by the Department of Defense.

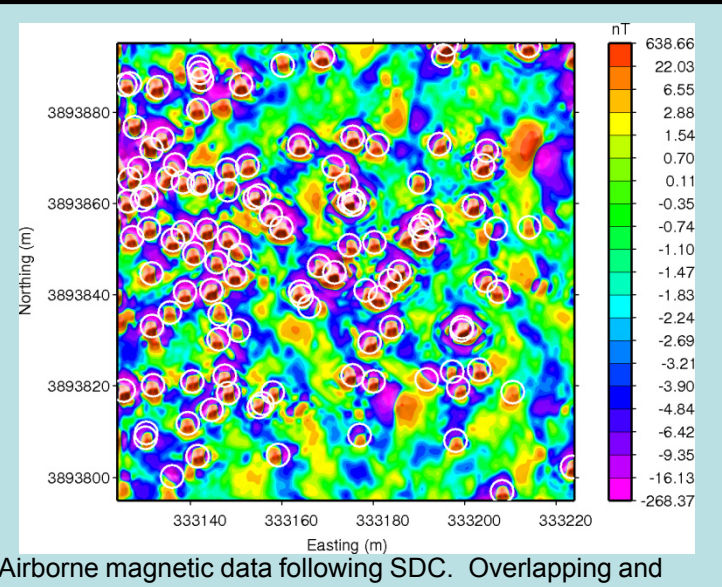
Enhancement of Magnetic Data by Stable Downward Continuation for UXO application



Enhancing the responses of two overlapping magnetic dipoles by stable downward continuation (SDC).



Airborne magnetic data from Kirtland AFB prior to SDC.
Targets selected by automated detection algorithm.



Airborne magnetic data following SDC. Overlapping and weak anomalies have been enhanced for improved detection.

Final Report SERDP SEED Project MM-1642

Yaoguo Li,
Richard Krahnenbuhl,
Sarah Devriese

Center for Gravity, Electrical, & Magnetic Studies
Department of Geophysics
Colorado School of Mines



Version 2
June 2010



SERDP
Strategic Environmental Research
and Development Program

EXECUTIVE SUMMARY

This is the final report for SERDP SEED Project MM-1642 and it covers the research results and developments for enhancement of magnetic data by stable downward continuation for UXO applications. The magnetic method is one of the two most effective geophysical techniques currently in use for UXO detection and discrimination. These data are always acquired with sensors at some height above ground surface, and it is well known that height significantly affects magnetic anomaly shape, amplitude, and spatial extent. Consequently, anomalies due to multiple metallic targets may overlap at a given height above the ground surface, and the acquisition noise may significantly decrease the signal-to-noise ratio (SNR) of data. These adverse effects ultimately mask the true level of contamination at a site during initial wide area assessment (WAA), as well decrease overall effectiveness of discrimination during the active clearance stage. The overall objective of the current project has therefore been to develop a robust algorithm for stable downward continuation (SDC) of magnetic data acquired at some height above the ground to reconstruct the magnetic data with a higher resolution at the ground surface.

The research performed over the first year of the project progressed satisfactorily with the major research tasks completed as scheduled and a working SDC algorithm developed and tested on synthetic and field data. The algorithm formulates the downward continuation as an inverse problem using Tikhonov regularization and has the flexibility of incorporating the expected power spectrum of UXO anomalies. The degree of regularization is estimated automatically using the well-established methods in linear inverse problems. Applications show that the algorithm can reliably estimate the noise in the data and reconstruct the magnetic anomaly at ground surface within the limitation imposed by the noise. The reconstructed field at the ground surface exhibits significant enhancement compared to the original data.

The second year of the project significantly advanced upon the original proposed research by incorporating an initial set of inversion algorithms to estimate the requisite ensemble depths within the data's radial power spectrum for improved SDC. In particular, development of recursive Quenched Simulated Annealing (QSA) from SERDP Project MM-1638 has been adapted for this purpose. The QSA algorithm has demonstrated a reliable tool for modeling the radial power spectrum of UXO magnetic data using non-linear parametric inversion. As a result, we can now automatically define a model objective function for SDC to quantify the conformity of the enhanced data with expected spectral properties.

In this report, we present the theoretical and practical aspects for development of stable downward continuation in UXO applications. We provide a means of estimating one's expected power spectrum within their UXO data through parametric inversion, and demonstrate successful application of SDC to synthetic and field data.

TABLE OF CONTENTS

EXECUTIVE SUMMARY	iii
LIST OF FIGURES	vii
LIST OF ACRONYMS	xi
ACKNOWLEDGEMENTS	xiii
CHAPTER 1 INTRODUCTION	1
1.1 SERDP Relevance	1
1.2 Technical Objective	2
1.3 Project Summary	3
CHAPTER 2 STABLE DOWNWARD CONTINUATION (SDC)	5
2.1 Introduction	5
2.2 SDC Algorithm	5
2.3 Power spectrum of magnetic data in UXO	9
2.4 Synthetic example	11
2.5 Summary	14
CHAPTER 3 POWER SPECTRUM ESTIMATION	15
3.1 Introduction	16
3.2 Quenched Simulated Annealing	18
3.3 Field example	21
3.4 Summary	21
CHAPTER 4 ANOMALY SEPARATION AND DATA ENHANCEMENT . .	25
4.1 Anomaly Separation and Limitation of SDC	25
4.2 Data Enhancement	28
4.3 Summary	31
CHAPTER 5 FIELD EXAMPLE	33
CHAPTER 6 SUMMARY	43
6.1 Proposed Research Accomplishments	44
6.2 Expanded Research Accomplishment	44
6.3 Future Research Recommendations	45

REFERENCES CITED	47
APPENDIX A PUBLICATIONS AND PRESENTATIONS	49
A.1 Publications	49
A.2 Presentations	49

LIST OF FIGURES

1.1	Airborne magnetic data collected from UXO site at Kirtland Air Force Base, NM. The data are in nanoTesla and it illustrates numerous overlapping anomalies from potential UXOs. The data clearly demonstrates the need for enhancing airborne magnetic data to suppress acquisition noise and separate overlapping anomalies.	2
2.1	Radially averaged power spectrum and its parametric representation. The blue curve is the numerically calculated power spectrum of a subset of magnetic data at Kirtland. The red line represents the radially averaged power spectrum and it consists of three distinct ensemble averages plus a constant noise power	11
2.2	Results of stable downward continuation applied to magnetic data generated for two closely spaced dipoles. The upper left panel is the original data with noise added. The upper right panel is the enhanced data from SDC processing. The lower left image is the predicted data at the original observation height, and it is a good fit to the original noisy data. The lower right panel is the noise estimate by subtracting the predicted and original data.	12
2.3	The top panels show respectively the data misfit (ϕ_d) and model objective function (ϕ_m) for the downward continuation shown in Figure 2.2. The Tikhonov curve in the lower-left panel has a well-defined corner that is located by the peak curvature point.	12
2.4	Comparison between the true anomaly at the ground surface and the stably downward continued anomaly for the example shown in Figure 2.2.	13
3.1	Manual fitting of example radial power spectrum of airborne magnetic data. The red-points are the true data calculated for the site. The solid-line is the predicted data by manual picking of ensemble parameters prior to stable downward continuation. The manual approach can adequately reproduce the general trend of the data; however, a better fit of the data can be achieved through robust inversion for the ensemble parameters.	20

3.2	QSA fitting of example radial power spectrum of airborne magnetic data. The red-points are the true data calculated for the site. The solid-line is the predicted data generated from QSA inversion for the seven unknown parameters in equation (3.3). Parametric inversion has significantly improved recovery of the three ensemble system over the manual approach from Figure 3.1	20
3.3	Airborne magnetic data collected over UXO site at Kirtland Air Force Base, NM. The data show high concentration of potential UXOs at the western end of the sub-grid, with numerous overlapping anomalies. . .	22
3.4	Radial power spectrum data calculated for the Kirtland AFB airborne magnetic data presented in Figure 3.3. The red-points are the true data calculated for the site. The solid-line is the predicted data generated from QSA inversion for the seven unknown parameters in equation (3.3). Parametric inversion has significantly improved recovery of the three ensemble system over the manual approach from Figure 3.1 . .	22
4.1	The cross-correlation coefficients between the stably downward continued anomaly and the true anomaly at the ground surface.	26
4.2	The observed data, produced at an observation height of 3 m with two dipoles buried at 0.5 m below the ground surface, is downward continued by 3 m. The result from data at this height do not have any indication of two separate anomalies, thus showing the limitations of the approach.	27
4.3	Comparison of the observations at two different heights (2.5 m and 3.0 m) above the ground surface, respectively, and the corresponding results of stable downward continuation.	27
4.4	A small subset of Kirtland airborne magnetic data.	29
4.5	Radial power spectrum of the Kirtland airborne magnetic data shown in Figure 4.4. The three ensembles correspond, respectively, to the surface magnetic soil and survey errors, UXO at the site, and a long-wavelength component possibly related to deeper geology.	30
4.6	Stable downward continuation of the Kirtland airborne magnetic data shown in Figure 4.4. The continuation process has reveal the presence of heading errors that were not completely removed by leveling of the original data. This indicates the need for further de-corrugation of the leveled data. More importantly, the continued data reveal clearly a number of dipolar anomalies (marked by circles) that were not apparent in the original data (Figure 4.4).	30

4.7	Comparison between downward continued data and ground observation. The dipolar anomalies marked by the circles in the upper panel were revealed by the downward continuation process, and they all correspond to the same anomalies shown in the ground magnetic data in the lower panel.	31
5.1	Figure from MM-0741 Report and associated caption indicating the area plan of the WAA survey and the locations of the HeliMag surveys. The data set presented in this chapter is from the Central South grid.	34
5.2	Airborne magnetic data acquired by HeliMag system of Sky Research, Inc. The data are located over the Central South grid as indicated in Figure 5.1	35
5.3	Data misfit, model objective function, and associated L-curve picking of the optimal regularization parameter for the stable downward continuation of the Kirtland data in Figure 5.2	36
5.4	Predicted data produced during the stable downward continuation of the data shown in Figure 5.2. This would be the de-noised data. They maintain the fidelity to the original data, and there is little visual indication of large differences.	37
5.5	Stably downward continued data of the Central South grid shown in Figure 5.2	38
5.6	(a) Automated Euler detection results from the original data in Figure 5.2. (b) Automated detection from SDC data shown in Figure 5.5 by using exactly the same parameters.	40
5.7	Detailed plots of northeast corner of the gird. (a) Automated Euler detection results from the original data. (b) Automated detection from SDC data.	41
5.8	Detailed plots of southwest corner of the gird. (a) Automated Euler detection results from the original data. (b) Automated detection from SDC data. Euler detection is able to capture nearly all of the dipolar anomalies from the SDC data.	42

LIST OF ACRONYMS

AFB - Air Force Base

ERDC - Engineer Research and Development Center

ESTCP - Environmental Security Technology Certification Program

FFT - Fast Fourier Transform

FUDS - Formerly Used Defense Sites

HE - High Explosive

lb - pound

m - meter

MM - Munitions Management

MTADS - Mobile Towed Array Detection SystemnT - nanoTesla

QSA - Quenched Simulated Annealing

SA - Simulated Annealing

SDC - Stable Downward Continuation

SEED - SERDP Exploratory Development

SERDP - Strategic Environmental Research and Development Program

SI - Structural Index

SNR - Signal-To-Noise Ratio

UXO - Unexploded Ordnance

WAA - Wide Area Assessment

ACKNOWLEDGEMENTS

The authors would like to thank SERDP, Dr. Jeffrey Marqusee, Dr. Anne Andrews, Dr. Herb Nelson, Ms. Katherine Kaye, and Mr. Peter Knowles for funding and support of the project. We also thank Steve Billings for discussion regarding the Kirtland HeliMag data.

We also acknowledge the help of Kristofer Davis for his contributions to the project. His efforts were instrumental in construction and editing of the final report, as well as running the automated target detection by extended Euler deconvolution to help validate the enhanced magnetic data following SDC processing.

CHAPTER 1

INTRODUCTION

1.1 SERDP Relevance

This project addresses the need for signal processing procedures as outlined in the Statement of Needs MMSEED-08-01, and seeks to develop a new technology for enhancing magnetic data by increasing data resolution and by estimating data noise for use in subsequent analyses.

The magnetic method is one of the two most effective geophysical techniques currently in use for UXO detection and discrimination. The use of magnetic data in UXO applications has been well studied and there are well-documented successful examples of locating and discriminating UXO. Detection of UXO through magnetic data depends on identifying dipole-like anomalies, while discrimination depends upon inversion to recover reliably the magnetic source parameters. These magnetic data are acquired with sensors at some height above ground surface. It is well known that height significantly affects magnetic anomaly shape, amplitude, and spatial extent. Consequently, anomalies due to multiple metallic targets may overlap at a given height above the ground surface, and the acquisition noise may significantly decrease the signal-to-noise ratio (SNR) of data. An example from Kirtland Air Force Base, NM (Billings et al., 2009), is presented in Figure 1.1. The data in this example are airborne magnetic data collected approximately 1 meter above the ground surface over a 281 m by 281 m grid and it demonstrates such overlapping anomalies and decreased SNR. These adverse effects will decrease the effectiveness of current detection and discrimination methods and may hamper the cost reduction of UXO clearance.

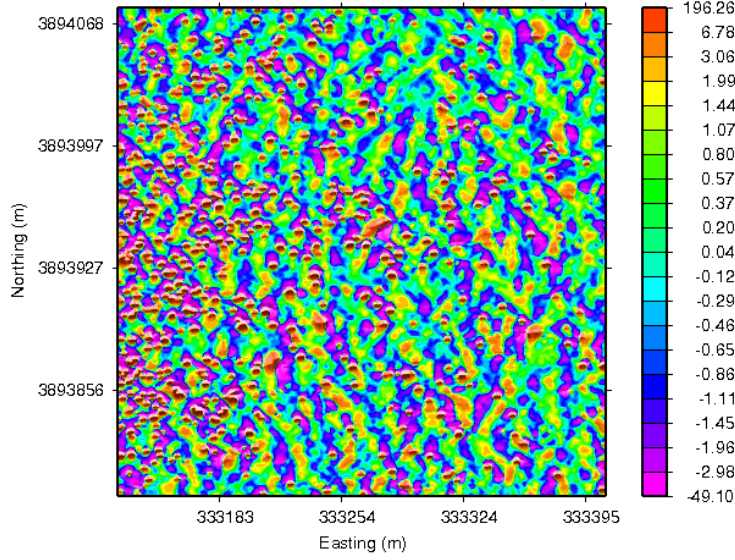


Figure 1.1. Airborne magnetic data collected from UXO site at Kirtland Air Force Base, NM. The data are in nanoTesla and it illustrates numerous overlapping anomalies from potential UXOs. The data clearly demonstrates the need for enhancing airborne magnetic data to suppress acquisition noise and separate overlapping anomalies.

1.2 Technical Objective

The purpose of this study is to develop a robust algorithm for stable downward continuation of magnetic data acquired at some height above the ground to reconstruct the magnetic data with a higher resolution at the ground surface, and also to characterize the noise in ground-based and airborne data. The specific objectives are:

1. Developing a robust algorithm for stable downward continuation of magnetic data;
2. Feasibility studies of application to airborne magnetic data, especially in wide area assessment (WAA) applications;
3. Feasibility studies of enhancing ground-based magnetic data; and
4. Noise estimation and its use in improved inversion algorithms.

1.3 Project Summary

In this report, we summarize the major research accomplishments of SERDP MM-1642 SEED Project. In short, we have accomplished the main objectives of this project, and we have made significant additional contributions to advance beyond the initial project goals.

In Chapter 2, we present the main development of stable downward continuation (SDC) for enhancing magnetic data in UXO applications. The algorithm is formulated as an inverse problem using a regularization approach, and it has been developed to incorporate the expected power spectrum of UXO anomalies. We expand beyond the original research goals of MM-1642 in Chapters 3. We have identified that there are distinct ensembles in all UXO magnetic data, and that we can efficiently recover the predicted power spectrum automatically through non-linear parametric inversion for these ensemble based models. This understanding has both theoretical implications and practical utility in processing UXO magnetic data and extracting anomalies. We have incorporated latest developments in Quenched Simulated Annealing from SERDP Project MM-1638 for this stage of of inverse problem.

In Chapter 4, we identify the parameters under which SDC may be able to increase the data resolution and gain an understanding of the limitations of the algorithm. We implement the algorithm on data sets to examine the data enhancement results, and to illustrate the possibility of using the algorithm to assess the noise in the data. Chapter 5 closes the research project with a series of large-scale field examples, demonstrating the effectiveness of SDC for enhancing airborne magnetic data from the ESTCP wide area assessment (WAA) demonstration project (MM-0741) at Kirtland Air Force Base.

We conclude the report in Chapters 6 and 7 with a discussion of the project developments, results, recommendations and publications/presentations generated throughout the lifespan of SERDP SEED Project MM-1642.

CHAPTER 2

STABLE DOWNWARD CONTINUATION (SDC)

2.1 Introduction

In this chapter, we present an algorithm for enhancing magnetic data in UXO applications using a stable downward continuation (SDC) method. The algorithm formulates the downward continuation as an inverse problem using Tikhonov regularization (Tikhonov and Arsenin, 1977) and has the flexibility of incorporating the expected power spectrum of UXO anomalies. The degree of regularization is estimated automatically using the well-established methods in linear inverse problems. Numerical tests show that the algorithm can reliably estimate the noise in the data and reconstruct the magnetic anomaly at ground surface within the limitation imposed by the noise. The reconstructed field at the ground surface exhibits significant enhancement compared to the original data. This chapter discusses the stable downward continuation algorithm, the estimation of expected power spectrum, the choice of regularization level, and demonstrates the method with a synthetic data set.

2.2 SDC Algorithm

The magnetic data at two observation heights are related by the upward continuation operation (Blakely, 1996),

$$T_h(x, y, \Delta h) = \frac{1}{2\pi} \int_{-\infty}^{\infty} \int_{-\infty}^{\infty} \frac{T_0(x', y') \Delta h}{[(x' - x)^2 + (y' - y)^2 + \Delta h^2]^{3/2}} dx' dy', \quad (2.1)$$

where $T_0(x, y)$ and $T_h(x, y, h)$ are respectively the magnetic data at two observation heights separated by a vertical distance Δh . Applying a two-dimensional Fourier transform to Equation (2.1) yields a simpler form in which the Fourier transforms of

the two quantities are related to each other by a simple upward continuation operator

$$\tilde{T}_h(\omega_x, \omega_y, \Delta h) = e^{-\Delta h \omega_r} \tilde{T}_0(\omega_x, \omega_y), \quad (2.2)$$

where $T_0(\omega_x, \omega_y)$ denotes the Fourier transform of $T_0(x, y)$, ω_x and ω_y are wavenumbers in x - and y -direction respectively, and $\omega_r = \sqrt{\omega_x^2 + \omega_y^2}$ is the radial wavenumber. The upward continuation operator attenuates the high-frequency content of a magnetic anomaly as a function of height. These effects can be partially reversed by performing downward continuation, which is the inverse of Equation (2.2), to reconstruct the field at the ground surface. The ground surface is the lowest possible observation height.

Although the operation of downward continuation is mathematically valid in the source free region above the ground surface (Blakely, 1996), it is numerically unstable because of the presence of high-frequency noise. However, we can stabilize the process by formulating it as an inverse problem and derive a regularized operator (Huestis and Parker, 1979). We will carry out this operation in the wavenumber domain because of the numerical efficiency.

Let us treat the Fourier transform $\tilde{T}_h(\omega_x, \omega_y, \Delta h)$ of observed magnetic anomaly at height Δh as the data, and the sought Fourier transform of anomaly at the ground surface as the model. The upward continuation operator $e^{-\Delta h \omega_r}$ then defines the forward mapping. The inverse problem is stated as finding a well-behaved $\tilde{T}_0(\omega_x, \omega_y)$ that has certain spectral characteristics and reasonably reproduces the data $\tilde{T}_h(\omega_x, \omega_y, \Delta h)$ by Equation (2.2). Assuming the magnetic data that would be observed at the ground surface has an expected power spectrum of $P_0(\omega_x, \omega_y)$, we can define a model objective function ϕ_m to quantify the conformity of the model with the expected spectral property,

$$\phi_m = \int \int P_0(\omega_x, \omega_y)^{-1} |\tilde{T}_0(\omega_x, \omega_y)|^2 d\omega_x d\omega_y, \quad (2.3)$$

where the reciprocal of the expected power spectrum provides the weighting function.

An assumed $P_0(\omega_x, \omega_y)$ that decays with increasing wavenumber corresponds to an increased weight at higher wavenumber for the final model. Consequently, the final model from the inversion will have the similar spectral decay. Such a spectral decay corresponds to a smooth magnetic field in the space domain. Thus, the use of inverse spectral decay as a weighting function provides a versatile approach to incorporate prior information about the magnetic data. We will discuss this aspect in more detail in the next section.

We define a data misfit function as,

$$\phi_d = \int \int |\tilde{T}_0(\omega_x, \omega_y) e^{-\Delta h \omega_r} - \tilde{T}_0(\omega_x, \omega_y, h)|^2 d\omega_x d\omega_y, \quad (2.4)$$

which is in effect the scaled version of data misfit in the space domain by Parseval's theorem. The lack of a normalization factor in this definition also implies the assumption of independent noise in the space domain, which translates to a constant noise level across the wavenumber band of the data.

Utilizing the formalism of Tikhonov regularization, the inverse problem of reconstructing the magnetic anomaly at the ground surface then becomes one of optimization:

$$\min : \phi = \phi_d + \mu \phi_m, \quad (2.5)$$

where μ is the regularization parameter and it determines the trade-off between fitting the data and the conformity of model with the expected spectral properties. Solving the minimization with the optimal value of regularization parameter μ produces the desired Fourier transform of downward continued data.

The solution of Equation (2.5) involves both complex data and a complex model. Therefore, we resort to the calculus of variation to carry out the formal minimization.

The result is a simple decoupled system and we have a closed-form inverse solution:

$$\tilde{T}_0(\omega_x, \omega_y) = \frac{e^{\Delta h \omega_R}}{1 + \mu P_0(\omega_x, \omega_y) e^{2\Delta h \omega_R}} \tilde{T}_h(\omega_x, \omega_y, \Delta h). \quad (2.6)$$

Performing a 2D inverse Fourier transform of $\tilde{T}_0(\omega_x, \omega_y)$ then yields the sought magnetic data at the ground surface.

The choice of regularization parameter μ determines the level of data fit and therefore the smoothness of the downward continued field. If we have precise knowledge of the statistics of errors in the data, we can define the expected value of the data misfit in Equation (2.4) and the optimal regularization parameter must be the one that yields the expected misfit. In general, we have little precise information about the noise characteristics, and this approach is not applicable. In such cases, we must resort to other methods to determine μ . The process then is equivalent to estimating the noise level in the data.

There are several approaches for performing the estimation. We apply the L-curve criterion (Hansen, 1992). The L-curve criterion is a heuristic method based on the behavior of Tikhonov curve. It was observed that, when plotted on a log-log scale, the data misfit as a function of model objective function exhibits a characteristic corner. As the degree of regularization decreases towards this corner point, the model objective function changes very little while the misfit is being reduced greatly. Further decrease in the degree of regularization beyond this point would result in rapid increase in the model complexity with little reduction in the data misfit. The L-curve criterion considers the corner point to be the best compromise between extracting maximum amount of signal and being least affected by noise. It therefore states that the optimal solution for a given regularized inverse problem is the one that corresponds to the corner point of the Tikhonov curve. The corner is defined numerically as the point with the maximum curvature.

2.3 Power spectrum of magnetic data in UXO

The formulation presented in the preceding section is general, and one can potentially use any assumed form of power spectrum to define the model objective function in order to stabilize the inversion. The weighting function based the reciprocal of assumed power spectrum has the ultimate effect of re-shaping the spectral content of the downward continued magnetic data. The faster decaying power spectrum corresponds to a smoother final result. For example, assuming $P_0 = \frac{1}{(\omega_x^2 + \omega_y^2)}$ is equivalent to requiring the downward continued data to be smooth by the first-order derivative in the space domain. In the absence of specific information regarding the nature of the source, such a generic assumption is useful for obtaining first order results. To obtain the best possible result, however, one must incorporate the correct spectral property consistent with the data set in question.

For our current application, we choose to use the theoretical radially averaged power spectrum. Consider a set of UXO items producing the magnetic data in question. Each UXO is represented by a magnetic dipole to a high degree of accuracy. Thus, we have an ensemble of random dipoles with varying dipole moments and burial depths. Spector and Grant (1970) showed elegantly that, within a scaling factor, the radially averaged power spectrum of the magnetic data produced by an ensemble is the same as that of the data produced by an "average" member of the ensemble. For a dipole source, this power spectrum has the following form,

$$P(\omega_r) \propto A\omega_r^2 e^{-2h\omega_r}, \quad (2.7)$$

where h denotes the vertical distance between the ensemble average and the observation plane and A is the scaling factor depending on the source strength. It follows naturally that we use Equation (2.7) to define the spectral weighting for enhancing magnetic data in UXO applications.

For practical applications, one must estimate the depth of the ensemble average

below the observation plane. This can be accomplished by performing a least-squares fit between Equation (2.7) and the radially averaged power spectrum of the data. To account for the presence of noise, we may also include a constant noise power to Equation (2.7). In general, the magnetic data are more complex than those produced by a single ensemble. For example, the magnetic soil will manifest itself in the data and exhibit as an ensemble at a depth near the ground surface. There could also be deeper geology at much greater depths below the UXOs. Thus, the power spectrum of a data set is typically consistent with that of multiple source ensembles, each having a different depth and source strengths. In addition, there is usually a random noise component. To obtain the correct power spectrum for use in the stable downward continuation algorithm, we must estimate these parameters numerically.

Once the average depth h of the UXO ensemble is obtained through this process, the power spectrum $P_0(\omega_x, \omega_y)$ used in defining the model objective function is given by

$$P_0(\omega_x, \omega_y) = \omega_r^2 e^{-2(h-\Delta h)\omega_r}, \quad (2.8)$$

where the vertical distance $h - \Delta h$ defines the ensemble depth below the ground surface to which we downward continue the data.

As an example, Figure 2.1 illustrates the power spectral estimation using a field data set from Kirtland Air force Base, NM. The blue line is the actual power spectrum calculated from the FFT of the magnetic data over a 30 m by 30 m area. The red line is the radially averaged power spectrum consisting of two distinct ensembles and a constant noise power. The first ensemble's average depth is consistent with the buried UXO in the area, and the second ensemble corresponds to the observation height above the ground. The agreement between the actual and theoretical power spectra with two ensembles is remarkable.

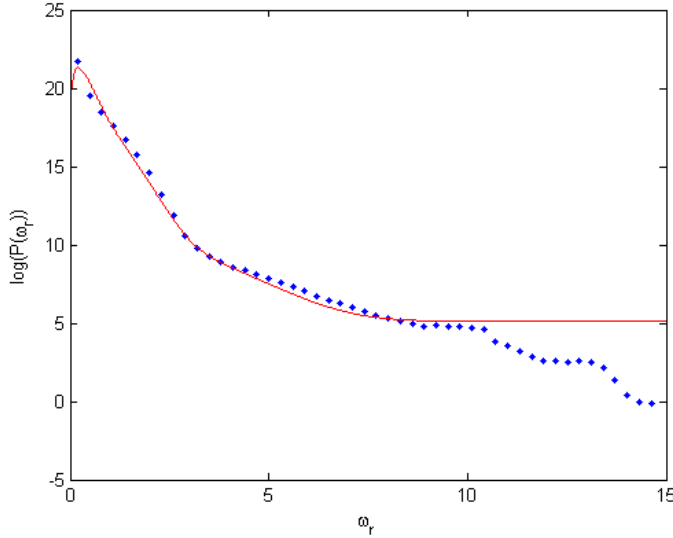


Figure 2.1. Radially averaged power spectrum and its parametric representation. The blue curve is the numerically calculated power spectrum of a subset of magnetic data at Kirtland. The red line represents the radially averaged power spectrum and it consists of three distinct ensemble averages plus a constant noise power

2.4 Synthetic example

We now proceed to illustrate the algorithm using a synthetic example. We first illustrate the details of the algorithm and show the effectiveness of the stable downward continuation. We then use this example to evaluate the range of observation height from which the enhancement is viable.

We use a model consisting of two buried dipoles separated horizontally by 2 m and buried at the same depth of 0.5 m below the surface. Assuming an observation height of 2 m above the ground surface and adding 0.5 nT of Gaussian noise, we simulated the observed data with 0.1-m spacing shown in Figure 2.2. At this height, the magnetic data shows one broad anomaly. In UXO applications, this might indicate the presence of clutters, but it would be difficult to discern how many buried targets are present.

Estimating a radial power spectrum and then applying the stable downward continuation yields the result shown in the same figure. The continued data are smooth

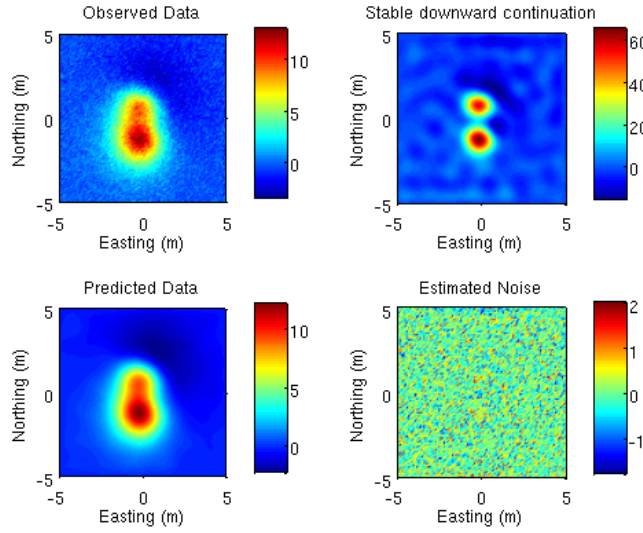


Figure 2.2. Results of stable downward continuation applied to magnetic data generated for two closely spaced dipoles. The upper left panel is the original data with noise added. The upper right panel is the enhanced data from SDC processing. The lower left image is the predicted data at the original observation height, and it is a good fit to the original noisy data. The lower right panel is the noise estimate by subtracting the predicted and original data.

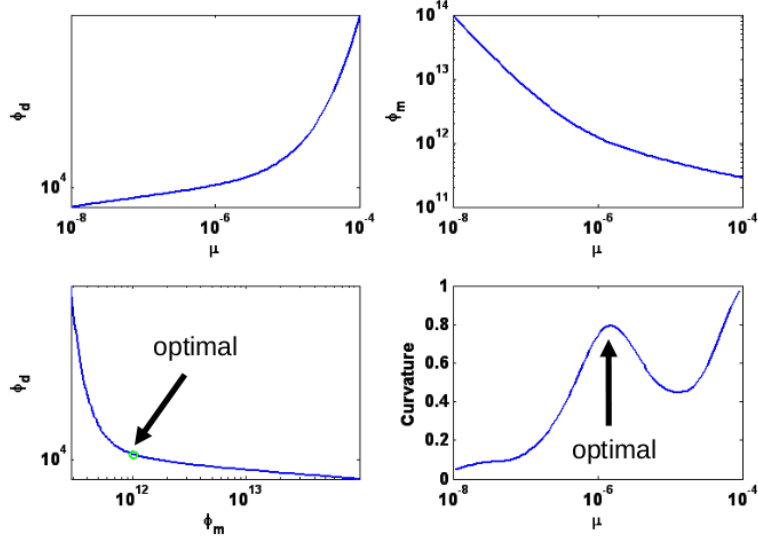


Figure 2.3. The top panels show respectively the data misfit (ϕ_d) and model objective function (ϕ_m) for the downward continuation shown in Figure 2.2. The Tikhonov curve in the lower-left panel has a well-defined corner that is located by the peak curvature point.

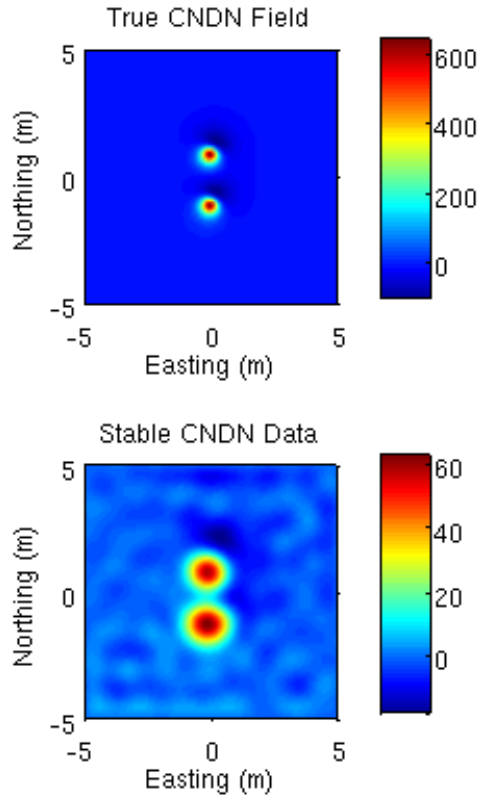


Figure 2.4. Comparison between the true anomaly at the ground surface and the stably downward continued anomaly for the example shown in Figure 2.2.

and well behaved. Two expected anomalies are clearly visible. For comparison, we also show the predicted data, which is a de-noised version of the observed data. The estimated noise given by the difference between the observed and predicted data is representative of the statistics of the actual noise.

Figure 2.3 shows more details regarding the performance of the algorithm. To search for an optimal regularization parameter, we have tested a range of values. The data misfit exhibits the typical monotonic increase with the regularization parameter, while the corresponding model objective function decreases monotonically. The Tikhonov curve has a well defined corner, as indicated by a single peak in curvature. This optimal regularization level yielded the result in Figure 2.2.

As a final assessment in this example, we compare the true anomaly from the two

dipoles at the ground surface with the downward continued data in Figure 2.4. We note that the downward continued data are smoother and the amplitude is greatly reduced. This is expected since the continuation process must attenuate a great deal of high-frequency content to obtain a stable solution. Despite the smooth appearance and low amplitude, the enhancement is significant since the two anomalies are clearly visible.

2.5 Summary

We have presented a stable downward continuation method for enhancing magnetic data acquired for UXO detection and discrimination. The key components are the expected power spectrum and automatic estimation of noise level in the data. The algorithm formulates the downward continuation as an inverse problem using Tikhonov regularization and has the flexibility of incorporating the expected power spectrum of UXO anomalies. The degree of regularization is estimated automatically using the well-established methods in linear inverse problems. Numerical tests show that the algorithm can reliably estimate the noise in the data and reconstruct the magnetic anomaly at ground surface within the limitation imposed by the noise.

In the next chapter, we present advances to the project beyond the proposed research, by identifying an ensemble based representation for UXO magnetic data, and by modifying recent inversion technologies to identify the expected spectral properties of this model representation as necessary for SDC.

CHAPTER 3

POWER SPECTRUM ESTIMATION

In the previous chapter, we demonstrated the approach of stable downward continuation to enhance magnetic data in UXO applications. The basic algorithm was developed and tested throughout the first year of the project. The two key components are the expected power spectrum and automatic estimation of noise level in the data. The second year of the project significantly advanced upon the original proposed research by incorporating an initial set of inversion algorithms to estimate the requisite ensemble depths and noise level within the data's radial power spectrum for improved SDC. In particular, development of recursive Quenched Simulated Annealing (QSA) from SERDP Project MM-1638 (Krahenbuhl et al., 2010) has been adapted for this purpose. The QSA algorithm has demonstrated a reliable tool for modeling the radial power spectrum of UXO magnetic data using non-linear parametric inversion. As a result, we can now automatically define a model objective function for SDC to quantify the conformity of the enhanced data with expected spectral properties. The procedure can be readily transferred for use in practice.

In this chapter, we provide a brief background on the power spectrum estimation problem, its formulation as a parametric inverse problem, solution by QSA. We also discuss the underlying ensemble models we have adopted in representing the power spectra of UXO magnetic data and its utility in understanding the source components of magnetic data. Although the estimation of the power spectrum is a basic component of the proposed work, what we have accomplished is a significant addition. The understanding achieved through the ensemble representation of magnetic data has both theoretical implications and practical utility in processing UXO magnetic data and extracting anomalies. We have observed that, in all UXO magnetic data we have examined, there are invariably distinct ensembles of magnetic sources present

and each ensemble has a good correspondence with a source group such as magnetic soil, UXOs, and underlying geology. This observation and understanding provide a practical and informative approach to examining magnetic data and separating signal components in UXO applications.

3.1 Introduction

For our current inverse problem, we have opted to use the theoretical radially averaged power spectrum. Consider a set of UXO items producing the magnetic data in question. Each UXO is represented by a magnetic dipole to a high degree of accuracy. Thus, we have an ensemble of random dipoles with varying dipole moments and burial depths. Spector and Grant (1970) showed elegantly that, within a scaling factor, the radially averaged power spectrum of the magnetic data produced by an ensemble is the same as that of the data produced by an "average" member of the ensemble. For a dipole source, this power spectrum has the following form,

$$P(\omega_r) \propto (A\omega_r^2 e^{-2h\omega_r}) + P_N, \quad (3.1)$$

where h denotes the vertical distance between the ensemble average and the observation plane, A is the scaling factor depending on the source strength, ω_r is the radial wavenumber, and P_N is a constant noise power. It follows naturally that we use Equation (3.1) to define the spectral weighting for enhancing magnetic data in UXO applications.

In general, one would expect there are other magnetic sources present at a given UXO site. Correspondingly, it would be reasonable to use multiple ensembles to represent the power spectrum of a data set. Indeed, we have observed this to be true in all data sets we have examined within this project and other related projects, such as MM-1638. At least three ensembles are present. The first tends to be associated with the soil magnetism and metallic objects scatter on the surface; the second associated

with UXO and other metallic objects buried in the ground; and the third with geologic responses at larger depth. The magnetic sources in the first two ensembles are depth limited and therefore has the dipole like behavior. Thus the form in Equation (3.1) is appropriate. The third ensemble, however, appears to be depth unlimited for the scale length relevant to UXO work. The corresponding radial power spectrum has the form of

$$P(\omega_r) \propto Ae^{-2h\omega_r}, \quad (3.2)$$

where the lack of the factor ω_r^2 describes the depth unlimited nature of the sources.

We have concluded in the project that the basic radial power spectral form should consist of four terms:

$$P(\omega_r) = A_1\omega_r^2 e^{-2h_1\omega_r} + A_2\omega_r^2 e^{-2h_2\omega_r} + A_3 e^{-2h_3\omega_r} + P_N. \quad (3.3)$$

Given this form, we structure the problem as a non-linear parametric inverse problem that seeks to recover the seven parameters ($A_1, A_2, A_3, h_1, h_2, h_3$, and P_N) for the three ensemble system. The associated objective function for the minimization problem is then expressed as the 2-norm difference between the logarithm of observed (\vec{d}^{obs}) and predicted radial power spectra(\vec{d}^{pre}):

$$\phi_d = \left\| \vec{d}^{obs} - \vec{d}^{pre} \right\|_2^2. \quad (3.4)$$

The procedure begins by performing fast Fourier transform (FFT) of the gridded magnetic data, compute the periodogram (square of the modulus of the FFT) as an approximation to the 2D power spectrum, and then then compute the radially average power spectrum. The use of logarithm is necessary since radial power spectra varies over many orders of magnitude.

Given the exponential and logarithmic functions involved in the objective function in Equation (3.3), this is a highly non-linear parameter estimation problem.

The solution to this parametric inverse problem is nontrivial. Although the standard Gauss-Newton approach (Nocedal and Wright, 1999) works to some extent, it usually requires significant user intervention in the form of initial guess to ensure that the minimization procedure starts within the convergence radius of the Gauss-Newton approach. To overcome this difficulty, we modify an optimization algorithm developed through SERDP Project MM-1638 for scanning the solution landscape. The method is a recursive Quenched Simulated Annealing (QSA) (Krahenbuhl et al., 2010), and we next present background information on QSA prior to demonstrating its application to the problem at hand.

3.2 Quenched Simulated Annealing

Simulated Annealing (SA) is global search technique (Kirkpatrick, 1984) well suited for non-linear parametric inversion such as we address in this project. SA formulation is designed to mimic the process of chemical annealing, where the final energy state of a crystal lattice is determined by its rate of cooling through the melting point. To achieve a lower energy state with highly ordered crystals, the material is usually cooled slowly. When the material is cooled too rapidly, the lattice may not reach the lowest possible energy state. The analogy in an inversion for this latter case is pre-mature convergence where the final solution has missed the desired global minimum. For geophysical inversion, the SA typically starts with a model at random, and calculates the model's energy based on its objective value as defined in the previous chapter. Perturbations are then applied to the model and the new objective values are calculated at each iteration. If the new objective value decreases or remains the same, the model is accepted as a replacement. If the objective value increases, the model is accepted by a thermally controlled probability function often referred to as the Metropolis criterion:

$$P = e^{(-\Delta\phi/T)}, \quad (3.5)$$

where $\Delta\phi$ is the difference between objective values of the old and new models, and T is a temperature parameter designed to decay (or cool) over time. For more information on SA, the reader is referred to Metropolis et al. (1953); Kirkpatrick (1984) and Nulton and Salamon (1988). Applications of SA specific to geophysical inversion are available in Sen et al. (1995); Nagihara and Hall (2001); Scales et al. (1992); Sambridge and Mosegaard (2002), and Martin et al. (2007).

We have opted to use a modified SA, called Quenched Simulated Annealing (QSA), as a local search tool for this (Krahenbuhl et al., 2010). QSA in its simplest form is Simulated Annealing described previously, without the Metropolis or any other cooling criteria such as Equation (3.5). The algorithm works as follows. After a change is performed to a model by QSA, i.e. one parameter is perturbed, the objective value of the new solution is calculated through Equation (3.4). If the change does not increase the total objective value the perturbation is accepted. Therefore, the algorithm only accepts downhill and lateral moves. Implemented recursively with random starting models, the method has a high likelihood of identifying any potential local minima within the solution space, as well as the desired global minimum.

As an illustration, we present the parameter fit to the power spectrum of a field data set. Figure 3.1 shows the manual fit to the data power spectrum (red dots) using the manually adjusted parameters (solid line). Note that we can reproduce the general shape of the power spectrum through this manual approach. However, as we illustrate next, recovery of the ensemble parameters in Equation (3.3) through robust inversion yields significant improvement over the manual approach.

Figure 3.2 demonstrates improved recovery of the three ensemble parameters for Kirtland over manual fitting. This is demonstrated by the well-resolved power spectrum (solid-line) in comparison to the true data (red-points). The high-quality fit of the data following inversion verifies that we have successfully recovered the expected spectral properties for the Kirtland AFB data.

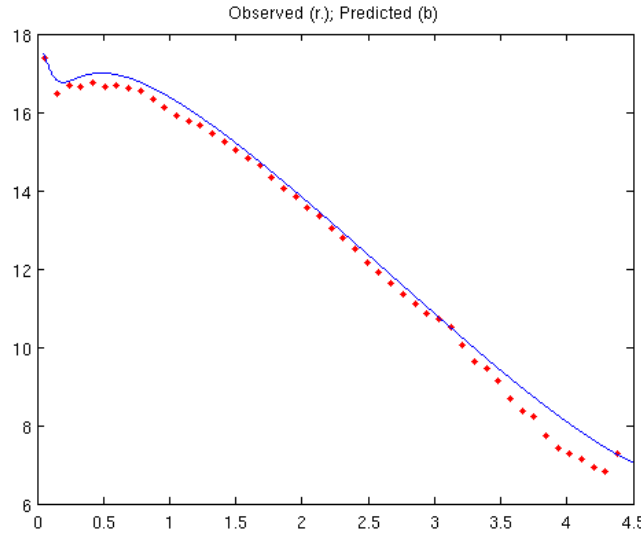


Figure 3.1. Manual fitting of example radial power spectrum of airborne magnetic data. The red-points are the true data calculated for the site. The solid-line is the predicted data by manual picking of ensemble parameters prior to stable downward continuation. The manual approach can adequately reproduce the general trend of the data; however, a better fit of the data can be achieved through robust inversion for the ensemble parameters.

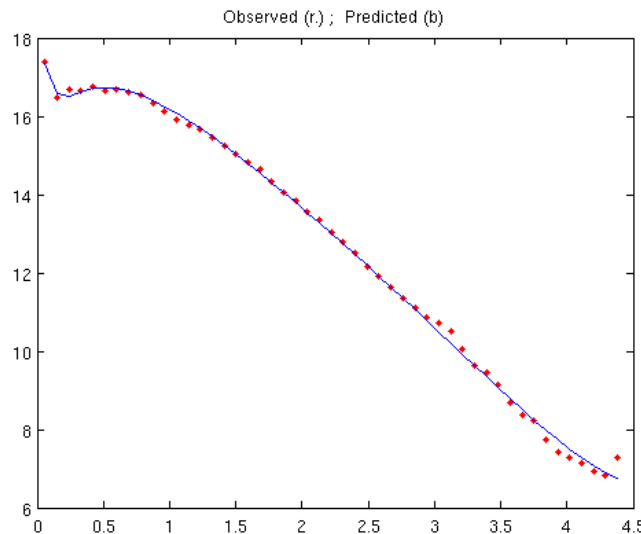


Figure 3.2. QSA fitting of example radial power spectrum of airborne magnetic data. The red-points are the true data calculated for the site. The solid-line is the predicted data generated from QSA inversion for the seven unknown parameters in equation (3.3). Parametric inversion has significantly improved recovery of the three ensemble system over the manual approach from Figure 3.1

3.3 Field example

We now present the result of power spectrum estimation using the three ensemble model applied to airborne magnetic data collected for UXO remediation efforts at Kirtland Air Force Base, NM (Billings et al., 2009). The original magnetic data, collected approximately one meter above the ground is presented in Figure 3.3. This is a subset of the entire data set. The data are gridded at an interval 0.25 m given the nominal 1-m line spacing.

The corresponding radial power spectral fitting is show in Figure 3.4. There are three distinct ensembles seen in the spectrum and a rather constant noise power is clearly seen in high-frequency band. We note that the gridding interval of 0.25 m could be slightly smaller than the data requires, because the fluctuation in the spectrum in the highest frequency band is clearly numerical noise.

The depths of the three ensembles below the data surface are respectively: 0.7, 2.5, and 11.5 m. We have interpreted these results as follows. The ensemble with a depth of 0.7 m corresponds to general noise in the survey, which consists of surficial variation of soil magnetism and clutters. Another source of the noise could be the altitude variation and positioning of the airborne platform. An average depth below the observation of 0.7 m, which is slightly above the ground, is quite reasonable. The second ensemble has an average depth of 2.5 m. Given the flight height of 1.0 to 1.25 m, this ensemble is about 1.25 m below the ground surface. This ensemble is precisely the expression of UXO and buried metallic objects detected in this survey. The third ensemble has an apparent depth of 11.5 m and it is reasonable to identify this group as geologic in origin.

3.4 Summary

In this section, we presented a method for automatically and reliably estimating the spectral properties of UXO magnetic data. The approach implements a recursive Quenched Simulated Annealing (QSA) leveraged from SERDP Project MM-1638,

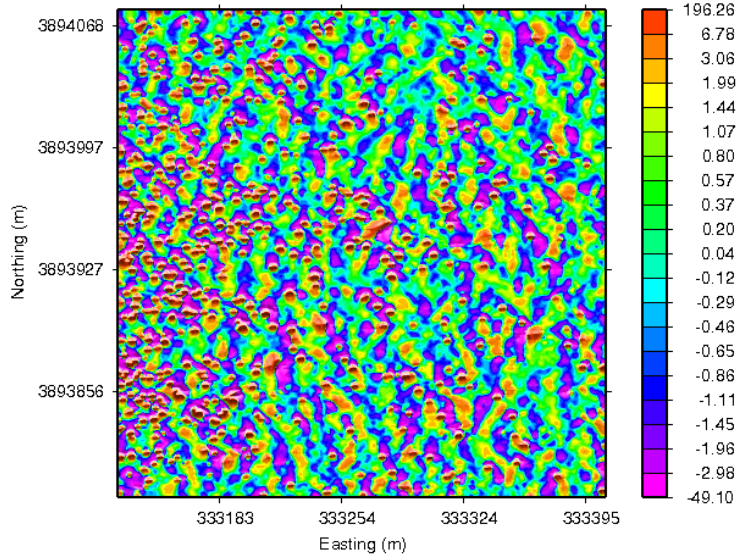


Figure 3.3. Airborne magnetic data collected over UXO site at Kirtland Air Force Base, NM. The data show high concentration of potential UXOs at the western end of the sub-grid, with numerous overlapping anomalies.

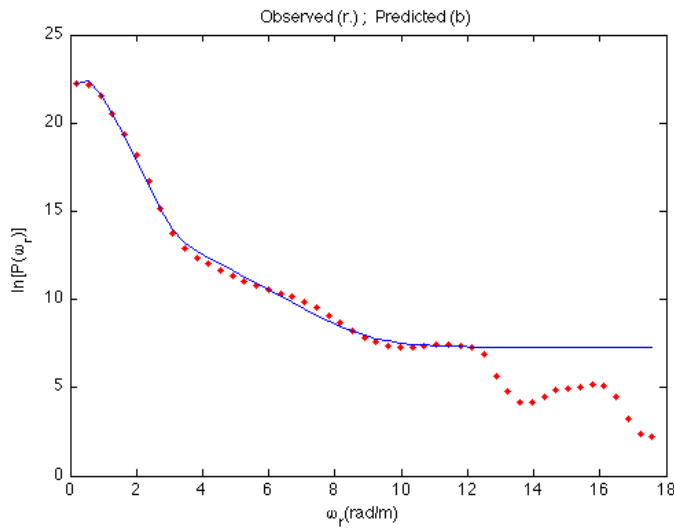


Figure 3.4. Radial power spectrum data calculated for the Kirtland AFB airborne magnetic data presented in Figure 3.3. The red-points are the true data calculated for the site. The solid-line is the predicted data generated from QSA inversion for the seven unknown parameters in equation (3.3). Parametric inversion has significantly improved recovery of the three ensemble system over the manual approach from Figure 3.1

and solves a non-linear parametric inverse problem to recover the seven parameters (including depths and noise power) of a three ensemble system. As a result of these developments, we can now automatically define a model objective function for stable downward continuation (SDC) to quantify the conformity of the enhanced data with expected spectral properties. In the next chapter, we apply the SDC approach to two data sets in order to understand the limitations of the algorithm, to demonstrate increased data resolution through SDC, and to evaluate SDC as a method for estimating noise in UXO magnetic data.

CHAPTER 4

ANOMALY SEPARATION AND DATA ENHANCEMENT

In this chapter, we apply the stable downward continuation algorithm developed in the preceding two data sets. The goals are to understand the performance of the algorithm and to evaluate the benefit that can be derived from the application of such an algorithm. The first data set is the synthetic data from the two-dipole model used in Chapter 2 and we will use it to investigate the parameters under which downward continuation may be able to increase the data resolution and gain an understanding of the limitations of the algorithm. The second data set is a small subset from the Kirtland WAA survey, and we use it to examine the data enhancement and illustrate the possibility of using the algorithm to assess the noise in the data.

4.1 Anomaly Separation and Limitation of SDC

We first return to the two-dipole model used previously and investigate the limit of the observation height from which the stable downward continuation can separate adjacent dipole anomalies. The ability to separate and distinguish adjacent anomalies ultimately determines the increased effective resolution of magnetic data for UXO detection.

We have carried out the simulation for a number of different observation heights in order to examine this aspect. The criterion is the ability to identify the presence of two separate anomalies from simulated observations at different heights. The two dipoles are buried at the depth of 0.5 m below the ground and separated by 2.0 m horizontally. We simulate data at observation heights ranging from 1 m to 3 m at an interval of 0.25 m. Gaussian random noise was added to each data set. The data sets are then stably downward continued to the ground surface by automatically choosing the optimal regularization parameter in each case. To assess the quality of downward

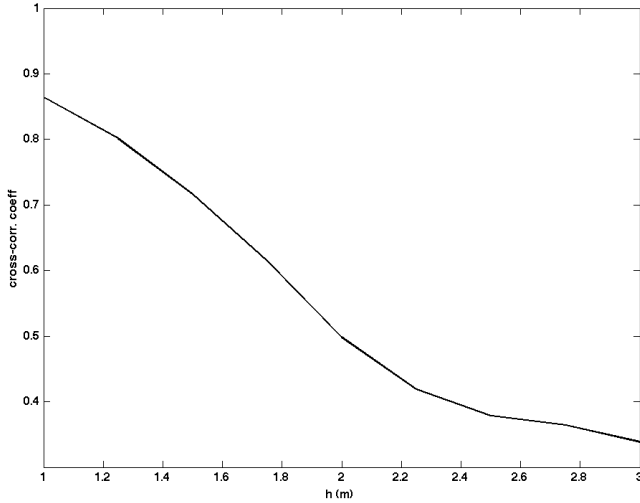


Figure 4.1. The cross-correlation coefficients between the stably downward continued anomaly and the true anomaly at the ground surface.

continued anomaly, we calculate its cross-correlation coefficient between the true magnetic anomaly at the ground surface. We also visually examine the continued field for the presence of two separate anomalies. Figure 4.1 displays the correlation coefficient as a function of the observation height. Visual inspection indicates that the continued anomaly shows two separate anomalies at a height equal to, or less than, 2.5 m. Correspondingly, we note that the correlation coefficient continues to decrease for observations above 2.5 m. This set of simulations therefore shows that the maximum observation from which we can enhance the magnetic data by stable downward continuation and discern two separate anomalies is 2.5 m. To illustrate this limit, Figure 4.2 shows the continuation result. The continuation result remains a single elongate anomaly and any detection algorithm will likely treat it as a single anomaly.

In the above case, the the maximum height is 2.5 m and the dipole depth is 0.5 m. The total distance between the observation plane and source is 3.0 m, which is 1.5 times the dipole separation. In general, this height depends on the dipole separation, noise level, and acquisition geometry. A higher signal to noise (SNR) of data would increase this height. Given the current quality of magnetic data in UXO application,

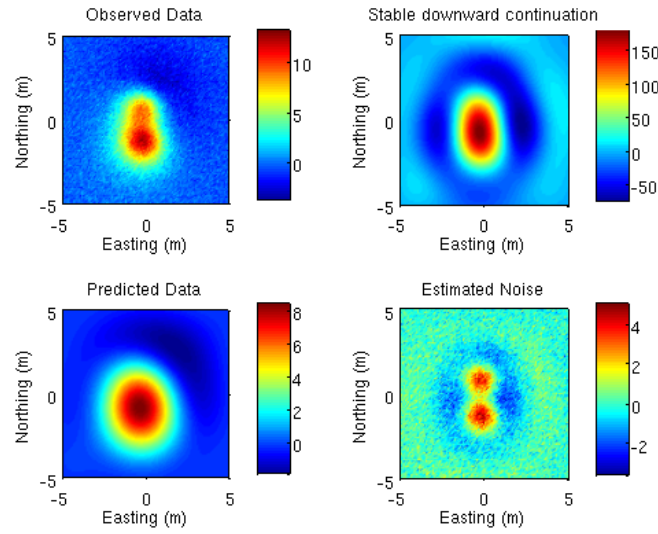


Figure 4.2. The observed data, produced at an observation height of 3 m with two dipoles buried at 0.5 m below the ground surface, is downward continued by 3 m. The result from data at this height do not have any indication of two separate anomalies, thus showing the limitations of the approach.

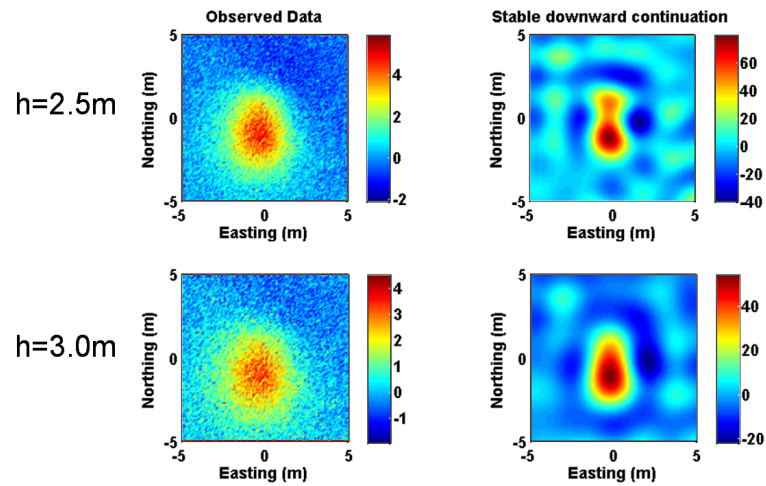


Figure 4.3. Comparison of the observations at two different heights (2.5 m and 3.0 m) above the ground surface, respectively, and the corresponding results of stable downward continuation.

however, we can infer that an observation height comparable to the dipole separation (1.0 to 1.5 times) is a reasonable limit.

4.2 Data Enhancement

We turn our attention to the application of SDC algorithm to field data and examine the potential enhancement from the continuation algorithm. We apply the method to a small subset of airborne magnetic data acquired from helicopter platform over Kirtland Air Force Base (Billings et al., 2009). We chose this subset because of the availability of ground magnetic data in the northern portion of this area. The overlapping data sets allows us to objectively assess the improvement in the continued data.

Figure 4.4 shows the data set over an area of 100 m by 100 m. The data have been gridded to an interval of 0.25 m in both directions. The radial power spectrum and its three-ensemble representation with noise component are displayed in Figure 4.5. Using this power spectrum to obtained the corresponding spectral weighting at 1.0 m below the observation height, we obtain the stably downward continued data shown in Figure 4.6.

Two observations can be made. First, there is significant striping in the east-west direction. This has been ascertained as the heading error in the original data. Although the data had been leveled during the post-acquisition processing, it is clear that the heading errors were not completely removed. Downward continuing the data has accentuated this component to the degree it is visible now. The heading error generally appears to be relatively high frequency in the cross line direction but long wavelengths in the flight direction. For this reason, the stable downward continuation tends to retain it in the result. The identification of the heading errors suggests that current practice in leveling of airborne magnetic data should be improved. This is especially important if data are to be used in discrimination process. Because of this observation, our subsequent work with field magnetic data has incorporated a step

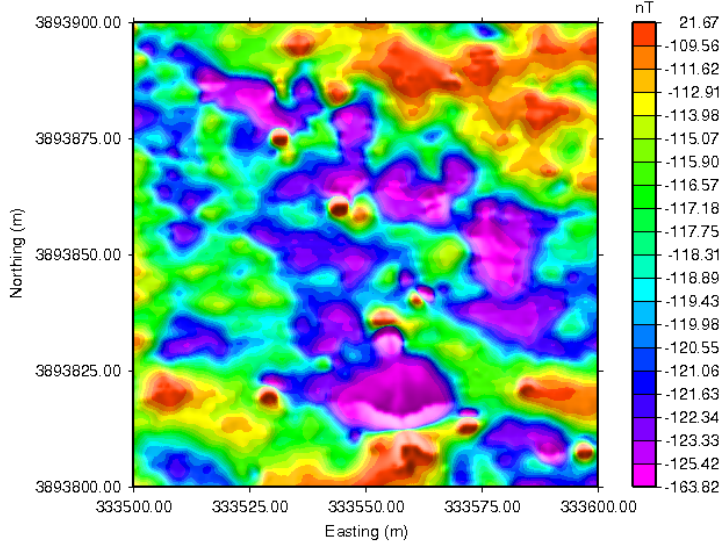


Figure 4.4. A small subset of Kirtland airborne magnetic data.

of micro-leveling to treat the heading error. Performing downward continuation after the required micro-leveling on Kirtland airborne data over large areas no longer show any noticeable heading errors. This will be exemplified in the following chapter.

The second observation is that the continued data are noticeably sharper and have accentuated higher frequency content. Several confined anomalies are now easily identified that were not clearly visible in the original data. The circles in Figure 4.6 mark several such anomalies. Each marked anomaly exhibits the dipolar pattern in the downward continued data, but they appeared in general as simple highs in the original data. The dipolar anomalies can be readily picked by a reliable automatic anomaly detection method.

We compare the downward continued airborne data with the ground magnetics in the same area in Figure 4.7. This is one of a few areas that have complete overlap between the airborne and ground data. Again we have marked the dipolar anomalies revealed by the downward continuation and the corresponding anomalies that are clearly visible in the ground data. Therefore, it is clear that the stable downward continuation has performed as expected in this case and is able to enhance the airborne magnetic data.

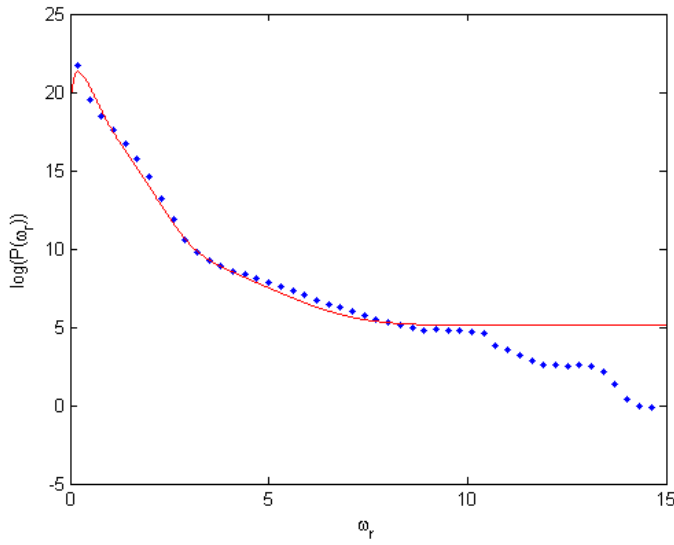


Figure 4.5. Radial power spectrum of the Kirtland airborne magnetic data shown in Figure 4.4. The three ensembles correspond, respectively, to the surface magnetic soil and survey errors, UXO at the site, and a long-wavelength component possibly related to deeper geology.

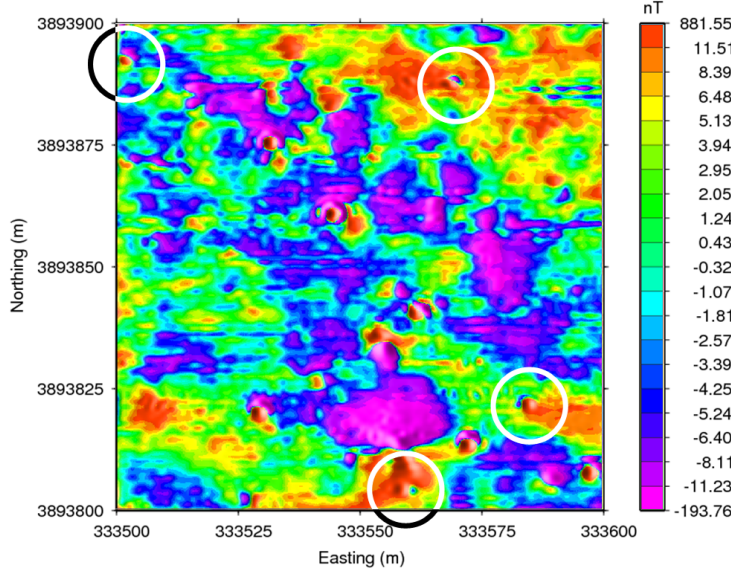


Figure 4.6. Stable downward continuation of the Kirtland airborne magnetic data shown in Figure 4.4. The continuation process has revealed the presence of heading errors that were not completely removed by leveling of the original data. This indicates the need for further de-correlation of the leveled data. More importantly, the continued data reveal clearly a number of dipolar anomalies (marked by circles) that were not apparent in the original data (Figure 4.4).

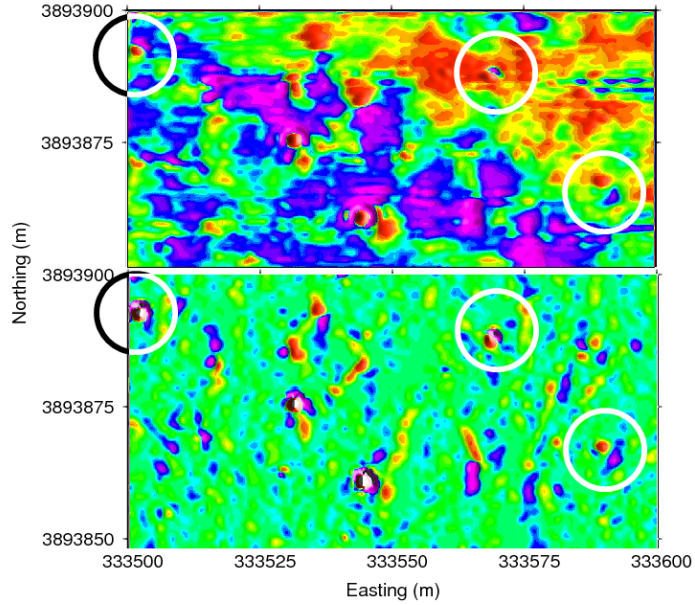


Figure 4.7. Comparison between downward continued data and ground observation. The dipolar anomalies marked by the circles in the upper panel were revealed by the downward continuation process, and they all correspond to the same anomalies shown in the ground magnetic data in the lower panel.

4.3 Summary

In this chapter, we have examined the potential enhancement of magnetic data using synthetic and field data sets. The first aspect is the enhancement of data resolution to distinguish between adjacent dipolar anomalies. We have concluded that when the observation height is comparable or slightly greater than the lateral separation of dipolar sources, it is possible with the current data quality to separate such anomalies through stable downward continuation. This puts the algorithm well within the parameter range of current helicopter-based airborne survey for UXO applications.

Application to a small subset of data from Kirtland Air Force Base clearly shows that several dipolar anomalies are revealed through the downward continuation process while controlling the noise magnification. Comparison with ground magnetic data show that the enhanced dipolar anomalies are real and correspond to the same anomalies present in the ground data. Thus, we have demonstrated the enhancement

of anomaly in actual data acquired for UXO applications.

An added benefit of the work is the identification of heading errors that exist in the leveled airborne data. Although such subtle error is not visible in the original data, stable downward continuation is able to identify it because of its long-wavelength nature along flight lines. Thus, further it is necessary to carry out de-correlation of such data prior to further analysis. In the next chapter, we conclude the project by applying the developed package and analyzing its performance to a series of large-scale HeliMag System data collected as part of the ESTCP wide area assessment (WAA) demonstration project (MM-0741) at Kirtland Air Force Base.

CHAPTER 5

FIELD EXAMPLE

The data analyzed in this chapter were acquired as a part of ESTCP wide area assessment (WAA) demonstration project (MM-0741) at the Kirtland Air Force Base west of the city of Albuquerque, New Mexico. ESTCP established a 6,500 acre demonstration sub-area for the WAA Pilot Program within the 15,246 acre FUDS. Documented ordnance at site includes M38A2 100-lb practice bombs, M85 100-lb practice bombs, and 250-lb general purpose HE bombs.

The airborne magnetic data were acquired using the HeliMag System operated by Sky Research, Inc. There are 13 sensors spaced 0.75 m apart on the platform. Flight lines were at 7 m to provide a 40% overlap. The altitude ranged from 1 to 3 m. Data density along track was one reading per 0.2 m (Billings et al., 2009).

We have processes four different areas within the survey. For brevity, we present the result from one area, which is the Central South grid shown in Figure 5.1 and covers approximately 300 m by 300 m.

Figure 5.2 displays the de-corrugated data after gridding to an interval of 0.25 m in both directions. The color bar corresponds to histogram equalized color contour intervals. Numerous localized anomalies are visible. This data set has been further processing using a de-corrugation filter to remove the residual heading error as observed in the preceding chapter.

We have stably downward continued these data by 1 m. Figure 5.3 shows the associated data misfit, model objective function, and choice of optimal regularization parameter by the L-curve criterion. The optimal the algorithm is able to pick the well-defined corner on the Tikhonov curve (lower left panel) as indicated by the single peak on the curvature. That is, the noise estimate in this case is quite reliable.

The predicted data, which constitute the de-noised data at the original observa-

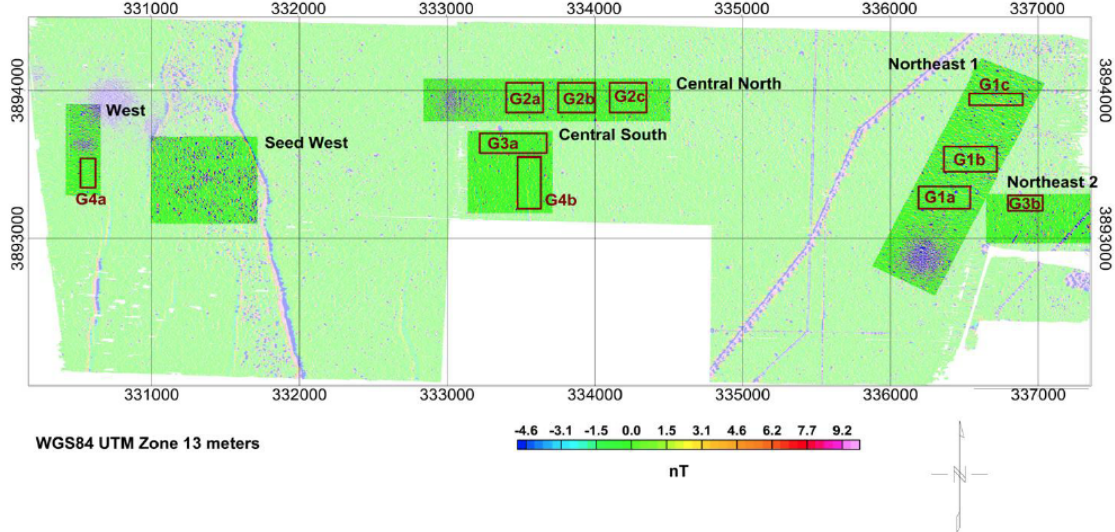


Figure 3. Overview of survey data collected.

The areas with opaque palettes were collected with the 13 sensor HeliMag configuration. The large semi-opaque palette is the AMTADS 2005 data set, and the boxes outlined in red represent areas that were surveyed with a ground-based towed magnetometer array in 2005.

Figure 5.1. Figure from MM-0741 Report and associated caption indicating the area plan of the WAA survey and the locations of the HeliMag surveys. The data set presented in this chapter is from the Central South grid.

tion surface, are shown in Figure 5.4. This set of data is a high fidelity representation of the original data and the difference ranges from -12 to 12 nT. At the scale displayed in the figure, little difference is visible. The downward continued data are displayed in Figure 5.5, which exhibit much greater amplitudes and most anomalies are visibly sharper. There is no longer visible stripping in the data due to the heading errors.

To verify the data enhancement gained through the stable downward continuation, we next apply an automated anomaly detection algorithm based on the extended Euler deconvolution (Davis and Li, 2010). The algorithm was developed initially with funding support from ERDC and SERDP projects MM-1414 and MM-1638. The automated detection solves for the structural index (SI) of each anomaly and treats those having an SI greater than a threshold as potential UXO (e.g. near 3) for metallic targets. A statistical analysis based on the amplitude-approximated source strength discard spurious solutions and the remainders are kept as target picks. A cluster algorithm based on proximity of these picks are then applied to group duplicate solutions

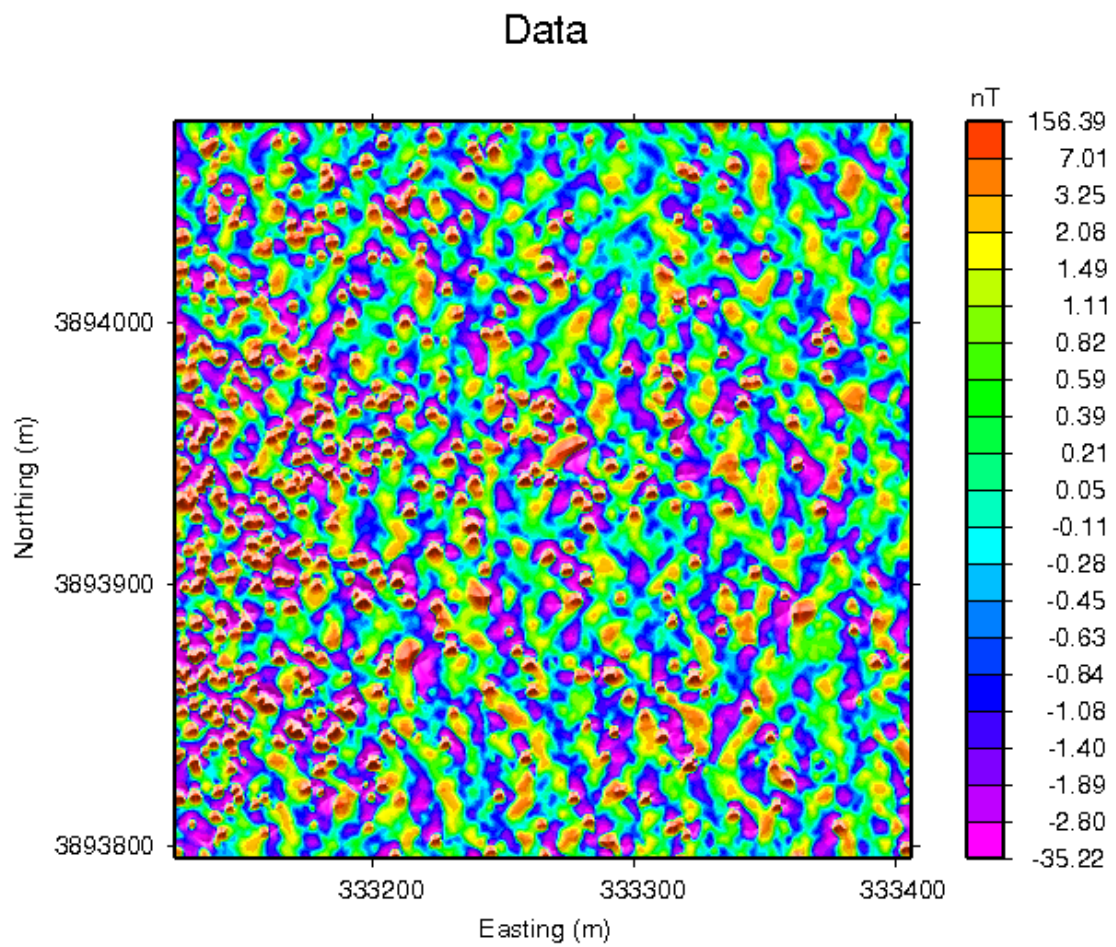


Figure 5.2. Airborne magnetic data acquired by HeliMag system of Sky Research, Inc. The data are located over the Central South grid as indicated in Figure 5.1

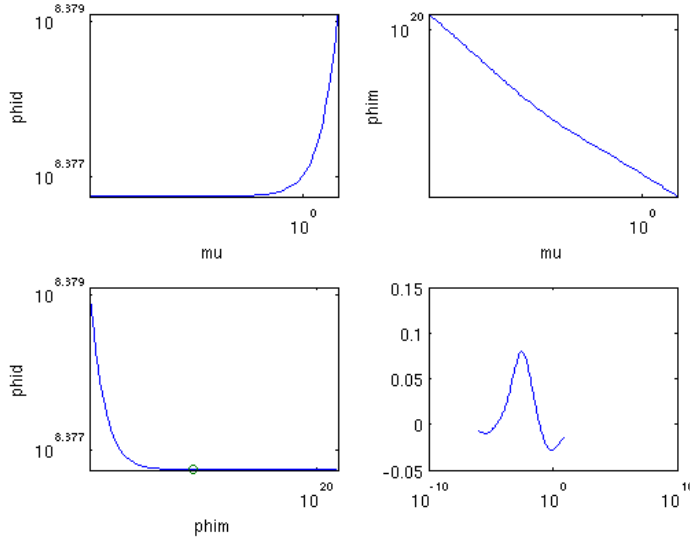


Figure 5.3. Data misfit, model objective function, and associated L-curve picking of the optimal regularization parameter for the stable downward continuation of the Kirtland data in Figure 5.2

into final picks. For the current data set, the SI threshold was chosen as 2.5 and the clustering distance was 1.0 m.

Figure 5.6(a) is the result of automated detection from the original de-corrugated airborne data, and Figure 5.6(b) shows the result from the downward continued data. Both plots have their respective data set as color images in the background and white circles denoting the target picks. The images cover the same area as the preceding data figures.

At first look, the two sets of results appear similar. However, closer inspection shows that there are two major differences. First, the results from SDC data have more individual anomalies picked, indicating the continuation indeed accentuated anomalies so that the detection algorithm is able to identify them. This is the same enhancement as illustrated through the small data set in the preceding chapter, where several broad anomalies are sharpened up to show their correspondence with the ground data. Secondly, the majority of the anomalies detected in the SDC data have single circles marking each of them, whereas the same anomalies in the original data

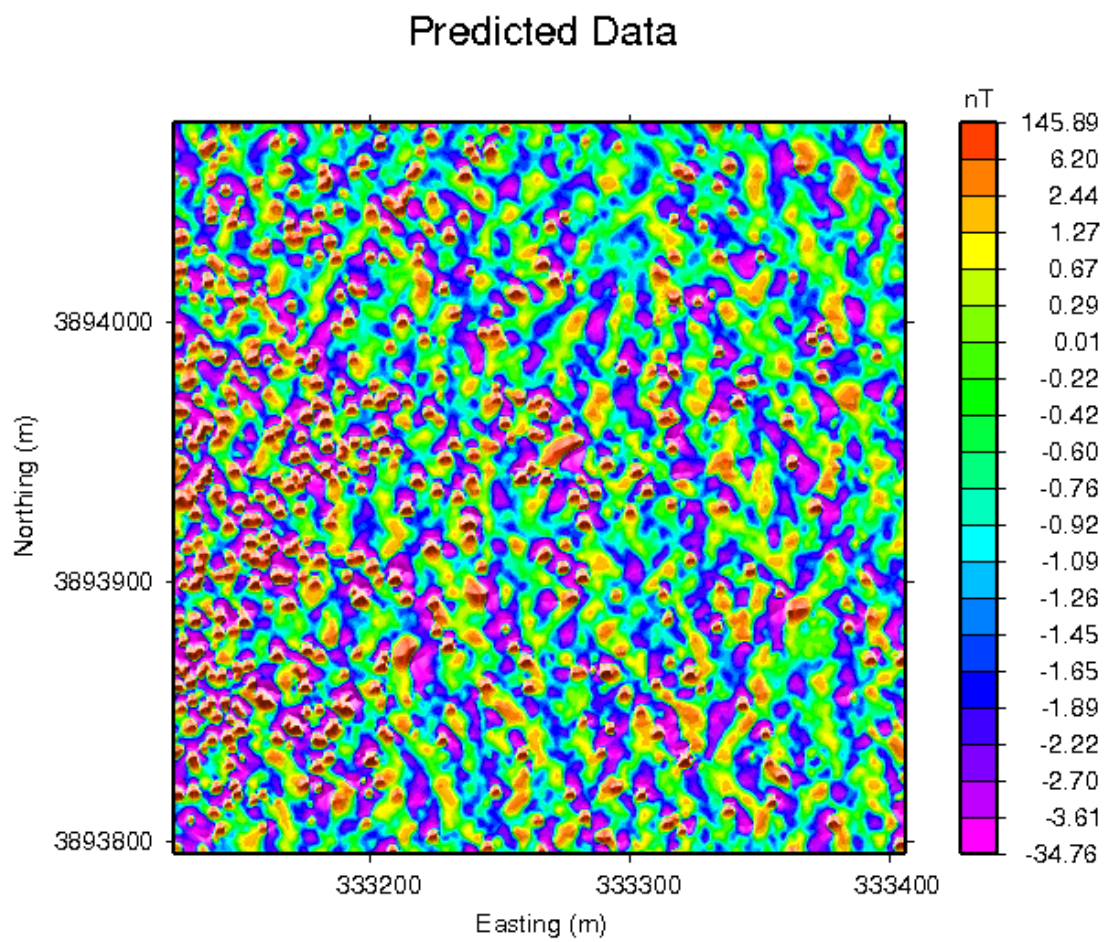


Figure 5.4. Predicted data produced during the stable downward continuation of of the data shown in Figure 5.2. This would be the de-noised data. They maintain the fidelity to the original data, and there is little visual indication of large differences.

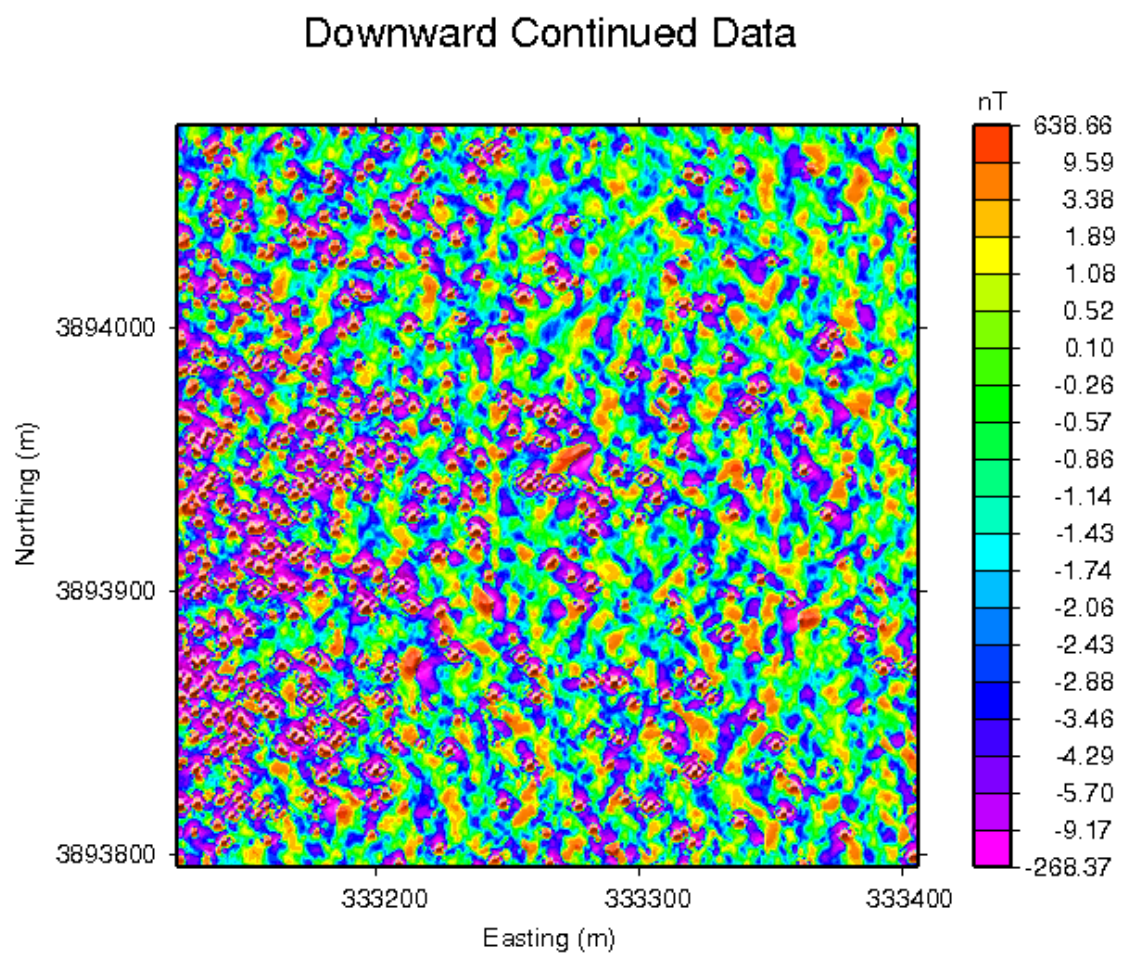
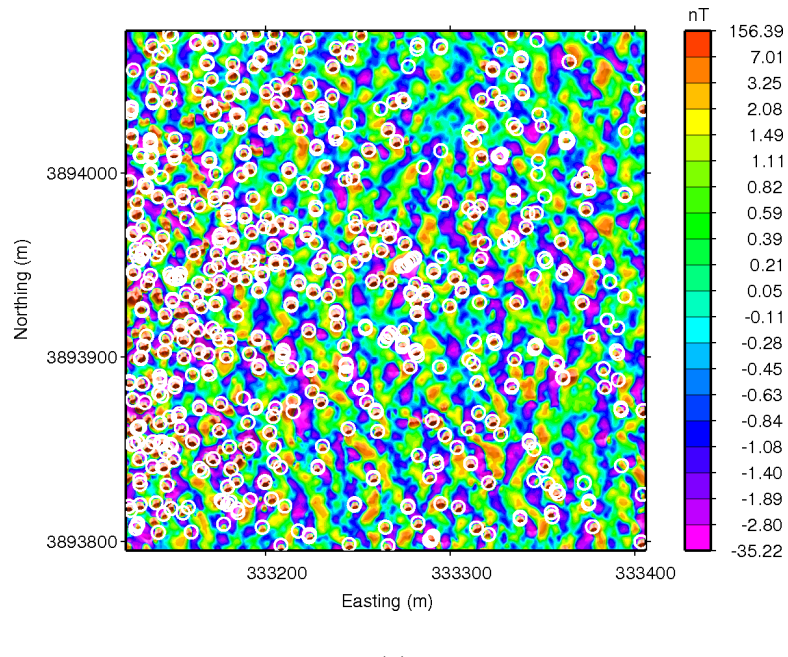


Figure 5.5. Stably downward continued data of the Central South grid shown in Figure 5.2

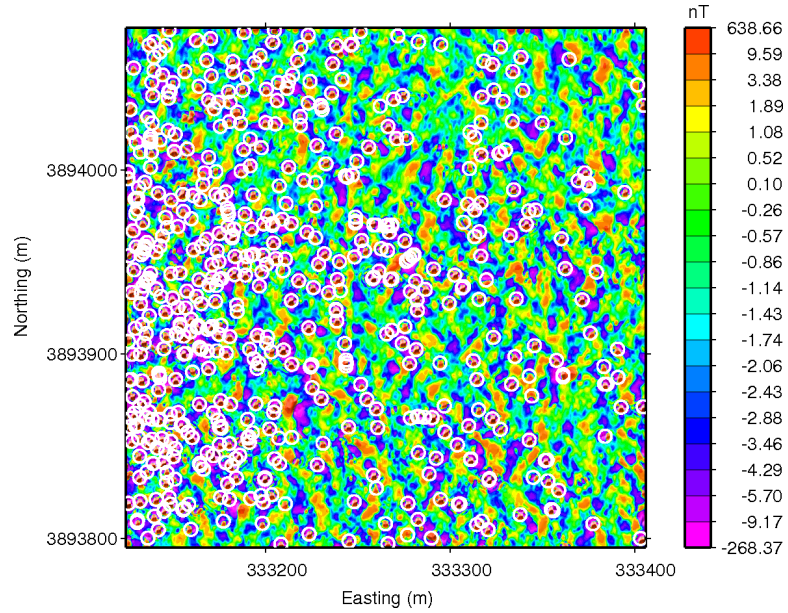
tend to have multiple circles that are slightly shifted from each other. That is, each anomaly in the original data has produced multiple picks. This occurs when the anomalies are broad and affected by noise. The enhanced anomalies through SDC are sharper due to the increased resolution and are less affected by noise. Therefore, the detection algorithm is able to produce much cleaner picks.

To illustrate these observations, we zoom in on two smaller areas within this grid to show more details. Figure 5.7 shows the comparison between detection results from the original data (a) and SDC data (b) in the northeast corner of the grid. This area has sparsely distributed dipolar anomalies. Primary improvement is indicated by mostly single picks for each anomaly in SDC. There are several occurrences where increased data resolution resulted in more picks, for example, towards the upper left corner, center of the map, and lower left corner.

Figure 5.8 shows a similar comparison between detection results from the original data (a) and SDC data (b) in the southwest corner of the grid. Many more dipolar anomalies are closely located, especially towards the west edge of the map. Because of the interference between adjacent anomalies in the airborne data, many of them are missed by the automated Euler detection algorithm. However, the stable downward continuation has significantly increased the resolution and enabled the separation of these anomalies. Consequently, the Euler detection is able to capture nearly all of the dipolar anomalies. It only missed three large-scale anomalies, each spanning over 10 to 15 m, which is much wider than the maximum window size of 5.25 m used in the detection. The difference displayed in this figure clearly demonstrates the enhancement which the stable downward continuation algorithm is able to produce.

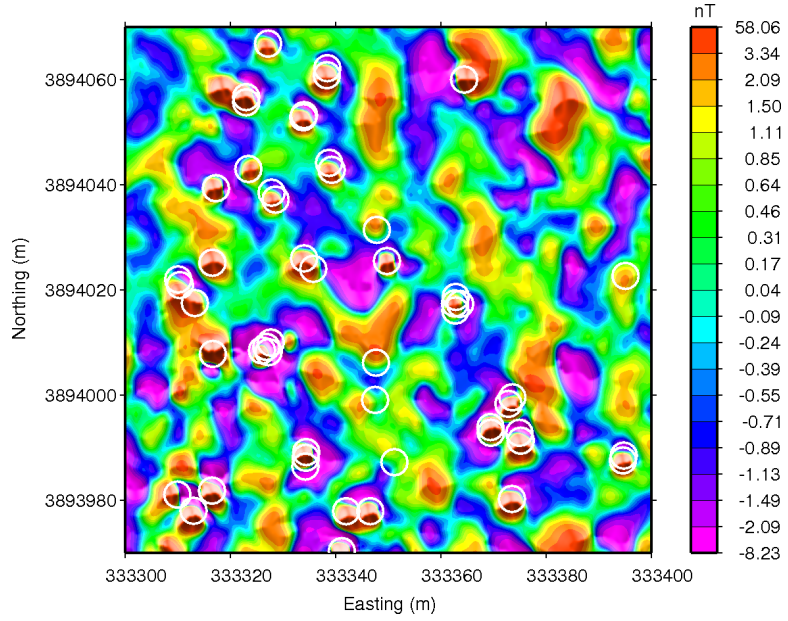


(a)

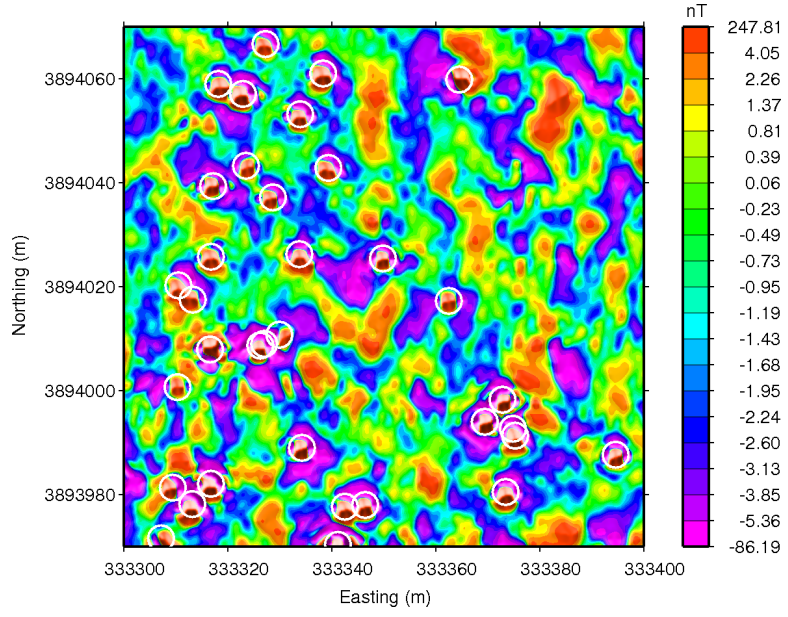


(b)

Figure 5.6. (a) Automated Euler detection results from the original data in Figure 5.2. (b) Automated detection from SDC data shown in Figure 5.5 by using exactly the same parameters.

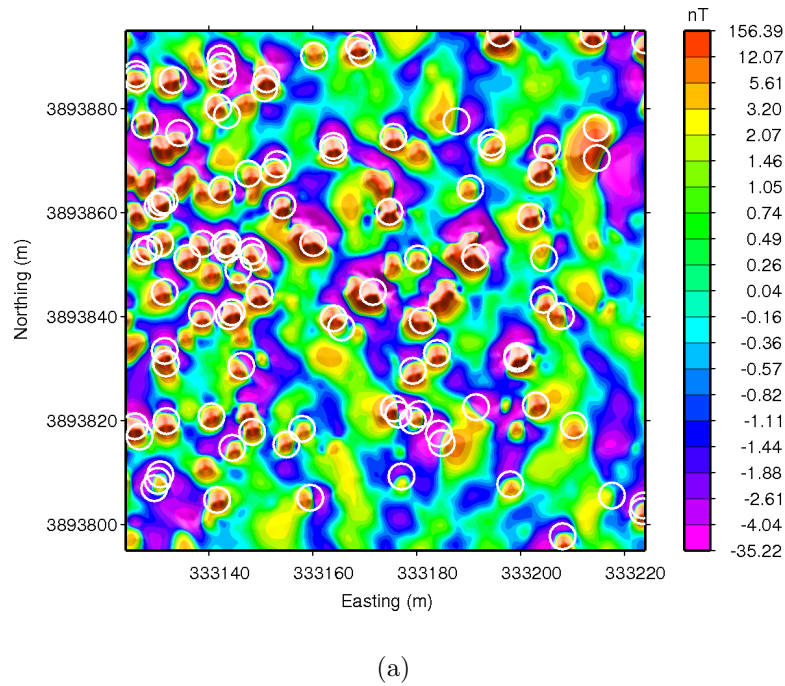


(a)

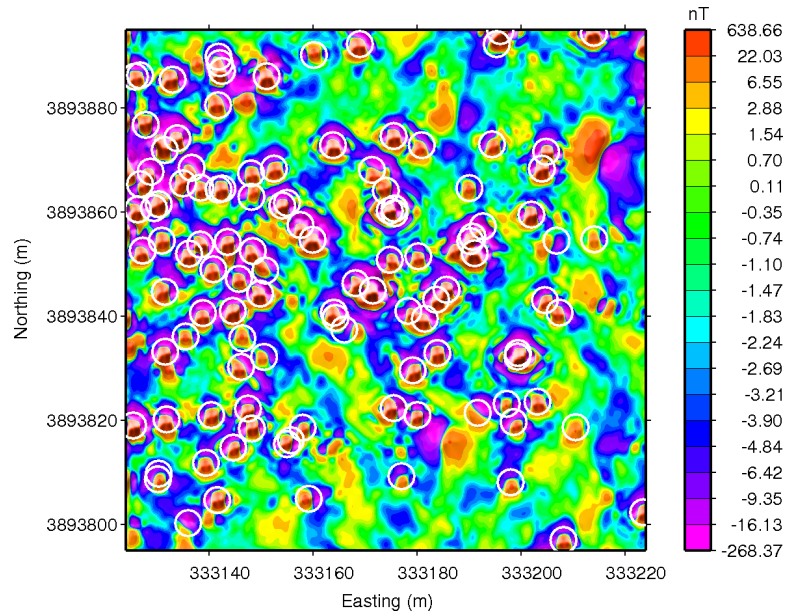


(b)

Figure 5.7. Detailed plots of northeast corner of the gird. (a) Automated Euler detection results from the original data. (b) Automated detection from SDC data.



(a)



(b)

Figure 5.8. Detailed plots of southwest corner of the gird. (a) Automated Euler detection results from the original data. (b) Automated detection from SDC data. Euler detection is able to capture nearly all of the dipolar anomalies from the SDC data.

CHAPTER 6

SUMMARY

Successful UXO discrimination is essential for minimizing the costs of ordnance clearance. Discrimination algorithms depend on accurate and reliable sensors for different types of data and the availability of high quality data these sensors provide. Much of the attention in UXO geophysics research has been devoted to the development of new sensors and new algorithms for data inversion and discrimination. However, a third and equally important aspect is the pre-processing of data and the extraction of data with high signal-to-noise ratio (SNR). Such algorithms provide a complementary component to newly-developed sensors and strengthen the foundation for advanced discrimination criteria.

The magnetic method is one of the most effective tools for UXO detection and discrimination. A great amount of data is being acquired using a variety of man-portable, vehicle-towed, and airborne platforms. The data are used in both discrimination for active clearance and wide area assessment (WAA) (e.g., ESTCP Project UX-0533). In particular, recent developments have enabled the recovery of dipole or ellipsoidal parameters through inversion of magnetic data (Billings, 2004). The reliability of these algorithms depends on well-defined anomalies associated with individual targets and a quantitative characterization of data noise.

The signal content and relative noise characteristics in a magnetic data set are strongly affected by the observation height. It is well known that the magnetic anomaly due to a dipolar source decays with distance cubed and the anomaly spreads out spatially in proportion to the distance as well. According to (Telford et al., 1990), for example, the width of a magnetic dipole anomaly at one half of its maximum is approximately equal to the source depth. This means that the data resolution defined as the distance between separable anomalies decrease linearly with increasing obser-

vation height and the relative noise in the data increase with the observation height. The ideal data are those acquired with a sensor at zero height above the ground. However, because of the intrinsic limitations imposed on field data acquisition, all previously-mentioned platforms collect data at some height above the ground surface. For example, the magnetic sensor height in a typical man-portable system or a vehicle-towed system (e.g., MTADS) may be between 0.15 to 0.5 m above the ground, and a helicopter-based survey would be flown at a height about 1.5 to 2.0 m above the ground (Doll et al., 2006). Thus, there is a need for enhancing magnetic data to alleviate the effects of observation height and to estimate the noise characteristics. This SEED project was established to address this specific aspect of magnetic data by developing and applying a stable downward continuation method.

6.1 Proposed Research Accomplishments

During the first year of the SEED project the main tasks were completed with a working SDC algorithm developed and tested on synthetic and field data. The algorithm, presented in Chapter 2, formulates downward continuation as an inverse problem using Tikhonov regularization and has the flexibility of incorporating the expected power spectrum of UXO anomalies. The degree of regularization for this formulation was estimated automatically using the well-established methods in linear inverse problems. Applications during the first year showed that the algorithm reliably estimates the noise in UXO data and reconstructs the magnetic anomaly at ground surface within the limitation imposed by the noise. The reconstructed field at the ground surface exhibits significant enhancement compared to the original data.

6.2 Expanded Research Accomplishment

The second year of the project significantly advanced upon the original proposed research by incorporating an initial set of inversion algorithms to estimate requisite ensemble depths within the data's radial power spectrum for improved SDC. These

developments are presented in Chapter 3 of the report. In particular, development of recursive Quenched Simulated Annealing (QSA) from SERDP Project MM-1638 has been adapted for this purpose. The QSA algorithm has demonstrated a reliable tool for modeling the radial power spectrum of UXO magnetic data using non-linear parametric inversion. As a result, we can now automatically define a model objective function for SDC to quantify the conformity of the enhanced data with expected spectral properties. In addition, we have been able to validate the SDC enhancement package over the last year by evaluating its performance with the latest detection technology based on the extended Euler deconvolution.

6.3 Future Research Recommendations

This project has demonstrated the validity of enhancing magnetic data using SDC and it is currently a well developed package for application in active UXO remediation efforts. However, there are still unanswered research questions necessary to complete development and understanding of the approach. The first question is understanding the effects and limitations of unavoidable variation in sensor height due to platform motion. This is particularly relevant for airborne systems implemented during WAA deployment. The second area is building an understanding of scale for practical implementation of SDC. We have identified through this project that magnetic data at UXO sites will require sectioning into sub-grids for proper data enhancement. A method must be developed that allows us to objectively identify sub-regions within the remediation site such that the data demonstrate similar spectral and statistical properties for effective SDC application. Finally, SDC method has demonstrated the potential, through ensemble based reconstruction of a model objective function, the ability to selectively downward continue data for enhanced data analysis. The natural result is that it is possible to expand the method into the realm of 'geology/background separation' algorithms needed in UXO remediation efforts, particularly for difficult data sets and environments. For example, it is likely

that SDC can contribute to the enhancement of difficult magnetic data at sites such as San Luis Obispo in California.

REFERENCES CITED

Billings, S. D., 2004, Discrimination and classification of buried unexploded ordnance using magnetometry: *IEEE Transactions on Geoscience and Remote Sensing*, **42**, 1241–1251.

Billings, S. D., D. Wright, J. Rogalla, and H. Nelson, 2009, Environmental Security Technology Certification Program (ESTCP) Cost and Performance Report. Next Generation HeliMag Mapping Technology. ESTCP Project MM-0741.

Blakely, R., 1996, *Potential theory in gravity and magnetic applications*: Cambridge University Press.

Davis, K., and Y. Li, 2010, Automatic detection of UXO magnetic anomalies using extended Euler deconvolution: *Geophysics*, **75**, no. 3, G13–G20.

Doll, W. E., T. J. Gamey, L. P. Beard, and D. T. Bell, 2006, Airborne vertical magnetic gradient for near-surface applications: *The Leading Edge*, **25**, no. 1, 50–53.

Hansen, P. C., 1992, Analysis of discrete ill-posed problems by means of the L-curve: *SIAM Review*, **34**, 561–580.

Huestis, S. P., and R. L. Parker, 1979, Upward and downward continuation as inverse problems: *Geophysical Journal of the Royal Astronomical Society*, **57**, 171–188.

Kirkpatrick, S., 1984, Optimization by simulated annealing: Quantitative studies: *Journal of Statistical Physics*, **34**, 975–986.

Krahenbuhl, R., Y. Li, M. N. Nabighian, K. Davis, and S. D. Billings, 2010, Advanced UXO detection and discrimination using magnetic data based on extended Euler deconvolution and shape identification through multipole moments: SERDP Project MM-1638 Annual Report.

Martin, A. G., J. R. Roy, L. Beaulieu, J. P. Pouliot, F. Harel, and E. Vigneault, 2007, Permanent prostate implant using high activity seeds and inverse planning with fast simulated annealing algorithm: A 12-year canadian experience: *International Journal of Radiation Oncology*Biology*Physics*, **67**, no. 2, 334–341.

Metropolis, N., A. W. Rosenbluth, M. N. Rosenbluth, A. H. Teller, and E. Teller, 1953, Equation of state calculations by fast computing machines: *Journal of Chemical Physics*, **21**, 1087–1092.

Nagihara, S., and S. A. Hall, 2001, Three-dimensional gravity inversion using simulated annealing: Constraints on the diapiric roots of allochthonous salt structures: *Geophysics*, **66**, 1438–1449.

Nocedal, J., and S. J. Wright, 1999, *Numerical optimization*: Springer Science.

Nulton, J. D., and P. Salamon, 1988, Statistical mechanics of combinatorial optimization: *Physical Review A*, **37**, 1351–1356.

Sambridge, M., and K. Mosegaard, 2002, Monte carlo methods in geophysical inverse problems: *Reviews of Geophysics*, **40**, no. 3, 3–1–3–29.

Scales, J. A., M. L. Smith, and T. L. Fischer, 1992, Global optimization methods for multimodal inverse problems: *Journal of Computational Physics*, **103**, no. 2, 258–268.

Sen, M. K., A. Datta-Gupta, P. L. Stoffa, L. W. Lake, and G. A. Pope, 1995, Stochastic reservoir modeling using simulated annealing and genetic algorithms: *SPE Formation Evaluation*, **10**, 49–56.

Spector, A., and F. S. Grant, 1970, Statistical models for interpreting aeromagnetic data: *Geophysics*, **35**, 293–302.

Telford, W. M., L. P. Geldart, and R. E. Sheriff, 1990, *Applied geophysics*: Cambridge University Press.

Tikhonov, A. N., and V. Y. Arsenin, 1977, *Solution of ill-posed problems*: Winston Press.

APPENDIX A

PUBLICATIONS AND PRESENTATIONS

A.1 Publications

Y. Li, Devries, S., and Krahnenbuhl, R., 2010, Enhancement of UXO magnetic data using stable downward continuation: Manuscript in preparation for submission to *Geophysics*.

A.2 Presentations

Li, Y., and S. Devries, 2009, Enhancement of magnetic data by stable downward continuation in UXO application: UXO/Countermine/Range Forum, Orlando, FL.

Li, Y., and S. Devries, 2009, Enhancement of magnetic data by stable downward continuation in UXO application: 79th Annual International Meeting of Society of Exploration Geophysicists, Houston, TX

Li, Y., and S. Devries, 2009, Enhancement of magnetic data by stable downward continuation in UXO application: SERDP-ESTCP Symposium, Washington, DC